Soil & Tillage Research 213 (2021) 105119

Contents lists available at ScienceDirect

Soil & Tillage Research

journal homepage: www.elsevier.com/locate/still

The role of cover crops in the loss of protected and non-protected soil organic carbon fractions due to water erosion in a Mediterranean olive grove

M. López-Vicente [d,1], J.A. Gómez [b], G. Guzmán [b], J. Calero [c], R. García-Ruiz [a,1,*]

[a] University of Jaen, Center for Advanced Studies in Olive Groves and Olive Oils, Campus Las Lagunillas s/n, Jaén, 23009, Spain
[b] Institute for Sustainable Agriculture, Agronomy Department, IAS-CSIC, Alameda del Obispo s/n, Córdoba, 14080, Spain
[c] University of Jaen, Department of Geology, Campus Las Lagunillas s/n, Jaén, 23009, Spain
[d] Advanced Scientific Research Center, University of A Coruña, CICA-UDC, Group Aquaterra. As Carballeiras s/n, Campus de Elviña, 15071 La Coruña, Spain

ARTICLE INFO

Keywords:
SOC
Spontaneous temporary cover crops
Soil erosion
Carbon enrichment ratio
Olive grove

ABSTRACT

Soil erosion plays an important role in C cycling at farm scale, especially in bare soil areas. In Mediterranean woody crops, temporary cover crops (CC) effectively reduce soil erosion and increase total and protected soil organic carbon (SOC) fractions. However, the effects of CC in olive groves on the preferential loss of organic carbon (C_{org}) fractions remains poorly understood. To address this issue, in four plots with seeded CC and two tilled plots (CT) in a Spanish olive grove, the unprotected and protected C_{org} fractions were measured in soil and sediments over the course of a hydrological year. The sediment/soil C enrichment ratios (ER_{SOC}) were calculated, and results analysed considering the rainfall regimes of the site: dry (DS), heavy-rainy (HRS) and rainy (RS). Total, unprotected and protected C_{org} contents in the top 5 cm soil of CC plots were 46 %, 88.4 % and 28.5 %, respectively, higher than those of CT. 79.7 % and 70.3 % of the annual sediment yield (SY) was collected during December in CC and CT plots, respectively. Soil loss in CC plots ($\bar{x}$ = 9.2 Mg ha^{-1} yr^{-1}) was significantly lower (−55.6 %) than that in CT plots. Despite that the average eroded C_{org} was higher in the CT ($\bar{x}$ = 222 kg C ha^{-1} yr^{-1}) compared to CC ($\bar{x}$ = 148 kg C ha^{-1} yr^{-1}) plots differences were not significant due to the higher C_{org} concentration in the sediment from CC plots. The highest proportion of eroded C_{org} (44%–45%) corresponded to the physically protected fraction. The highest ER_{SOC} (1.99 and 2.04 for CC and CT, respectively) was recorded in DS whereas the lowest was in the RS (0.90) and HRS (0.96) seasons. The mean ER_{SOC} were of 1.00 and 0.92 in the CC and CT plots, with no significant difference. The fact that most of the SY was recorded in one month, when CC plants were not fully developed, might explain the ER_{SOC} at 1, and why their presence did not modify it. This study demonstrates that CC favours greater total, unprotected and protected C_{org} fractions in the topsoil, promoting soil C sequestration. The asynchrony between the periods of full development of the CC plants and those with the highest rainfall erosivity prevented any selectiveness of the eroded C_{org}. Thus, fast-growing CC plant species with short life-cycles are recommended, as well as adequate management to promote self-seeding avoiding soil disturbance for seeding in erosion prone seasons.

1. Introduction

The role of soil erosion in croplands as a net source or sink for atmospheric carbon (C) at regional and global scales is currently being debated (Stockmann et al., 2013; Borrelli et al., 2018; Naipal et al., 2018). Lal (2003) estimated the global erosion-induced displacement of soil organic carbon (SOC) at 5.7 Pg C yr^{-1}, and of that amount, approximately 70 % is redistributed and redeposited over the landscape whereas the remaining 30 % is transported by rivers into aquatic ecosystems. At farm level, numerous studies point out that this complex process is associated with a decline in SOC content (Xiao et al., 2018; Jian et al., 2020). Indeed, being concentrated near the soil surface, SOC is drastically impacted by erosion processes, and many studies on soil erosion-carbon relationships have reported high losses of SOC on eroded

* Corresponding author.
E-mail address: rgarcia@ujaen.es (R. García-Ruiz).
[1] These authors contributed equally to this study.

https://doi.org/10.1016/j.still.2021.105119
Received 3 December 2020; Received in revised form 10 June 2021; Accepted 18 June 2021

sites (e.g. Lal, 2019; Rolando et al., 2017; Wang et al., 2017a, b). On a global scale and over the last century, it is estimated that around 42–78 Gt of C have been lost due to inappropriate soil management practices and soil erosion (Paustian et al., 2000; Lal, 2004). In the European Union cropland soils, the loss of SOC induced by erosion has been similar to that gained after improved management practices (Lugato et al., 2016). Roose and Barthes (2006), after reviewing 54 runoff plots, found values of eroded organic carbon of between 50–400 kg C ha^{-1} yr^{-1} for cereals and cotton in humid and sub-humid regions and some bare plots in Mediterranean regions, and up to 3 Mg C ha^{-1} yr^{-1} for bare tilled soils in very humid regions. These authors highlighted that the relative importance of eroded SOC in C budgets was paramount on tilled plots. However, the effects of soil erosion and the fate of the specific SOC fraction transported by overland flow remains poorly understood.

The '4 per 1000' Initiative –launched by France on 1 December 2015 at the COP 21– aims to increase global soil organic matter, and thus, organic carbon stocks by 0.4 % per year as a compensation for the global emission of greenhouse gases by anthropogenic sources (Minasny et al., 2017). This declaration set up a conceptual framework under whose umbrella research on technically and economically feasible management practices that can contribute to a positive net balance of SOC has intensified. Among these practices, those aimed to lowering soil erosion have gained special emphasis (Sykes et al., 2020). Thus, policy makers face the challenge of developing and implementing effective SOC accretion strategies for agriculture, which require identification of the best management practices for each type of agroecosystem (Ogle et al., 2019) as well as adequate quantification of its impact.

Olive tree is one of the most important woody crops in the Mediterranean region, not only for the large area it occupies (>10 Mha), but also for shaping the socio-economical life in many rural areas (Beaufoy, 2001). In Andalusia (Southern Spain), about 47 % of the agrarian territory is planted with olive trees, and therefore, management practices affecting the SOC dynamics might have important effects on organic carbon budget at regional scale and on the C footprint in the olive oil sector. Typically, olive cultivation has been accompanied by accelerated erosion and soil degradation (e.g. Beaufoy, 2001; Scheidel and Krausmann, 2011), as olives have been traditionally cultivated under rainfed conditions on sloping areas, at relatively low tree density, with limited canopy size by pruning and bare soil management to adapt to a water limited environment (Gómez et al., 2011). Some estimates of historical soil erosion in olive groves exceed the tolerable soil loss rates in cultivated soils (between 1.26 and 4.69 Mg ha^{-1} yr^{-1}; Vanwalleghem et al., 2011). In the latest decade, studies have started to deepen our understanding about the relationships among soil erosion and SOC in olive orchards (Gómez et al., 2009, 2017, 2020).

The implementation of temporary cover crops (CC) during the growing season in woody crops, such as olive groves or vineyards, is a sustainable and efficient management practice to harmonize agronomic requirements and reduction of soil erosion, and thus, SOC loss (Francia-Martínez et al., 2006; Gómez et al., 2009; Guzmán et al., 2019a). CC in woody crops also favour transferring atmospheric C to the soil and have an active role in the stabilization of SOC, by providing plant-residue-derived organic carbon (Vicente-Vicente et al., 2016; Almagro et al., 2017; Novara et al., 2019). This is an important issue in Southern Spain, where regional authorities introduced a policy of Standards of Good Agricultural and Environmental Conditions within the European Common Agricultural Policy requirements in olive farming, which consists of linking the economic subsidy for cultivating the olive crop to the requirement of providing/ permitting CC under certain circumstances (mean slope gradient over 10 %). CC in olive oil orchards are mainly comprised of natural vegetation, which is allowed to emerge spontaneously in autumn and winter along the middle of the orchard lanes. Under Mediterranean climatic conditions, CC in permanent crops are usually terminated in late March or early April, before competing for water and also nutrients what would end up reducing crop yield. This CC control is mainly based on mechanical mowing and/ or herbicide application (Ben-Salem et al., 2018). Plant residues may be left on the soil surface or mixed into the topsoil by tillage. Both approaches are currently used and are realistic land management options. Most previous studies related to the effectiveness of CC in olive orchards have been designed to evaluate the effects of this practice in mitigating soil erosion (e.g. Gómez et al., 2009, 2011, 2018a, b), but to a lesser extent to evaluate the reduction in total SOC loss or in some of the unprotected or protected fractions.

Vicente-Vicente et al. (2017) demonstrated that CC induced a change in the content of the different SOC fractions in the soil, as they found in olive groves of Andalusia. In particular, these authors observed that spontaneous temporary CC increased SOC, especially the coarse non-protected fraction, and the physically and chemically protected SOC of the top 15 cm of soil. On the other hand, the eroded soil includes detaching of soil particles from clods, breakdown of macro into micro-aggregates and dispersion into soil separates and transporting particles (sediments hereafter) over soil surface. Depending on many factors, which include the content of stable macro-aggregates, particles' density and weight and runoff transport capacity –all of them affected by the presence of temporary CC and plant residues–, there is a selective preferential loss of soil and detritus particles, and thus, of SOC fractions, from the eroded to the depositional sites. For instance, Wiaux et al. (2014) and more recently Li et al. (2019), found that non-resistant to NaClO (e.g. labile) and fast SOC pool were preferentially transported from the eroded areas. Despite temporary CC play a crucial role in: I) the increase of total SOC and specific SOC fractions of different protective degrees, and II) the factors that control the selectiveness of the eroded sediment, the effect of temporary CC in olive groves on the preferential loss of specific SOC fractions during the different seasons –or rainfall regimes– remains poorly understood.

Translocation of organic rich topsoil material from eroding to depositional sites explains the sediment/soil C enrichment ratios (ER_{SOC}) (Wang et al., 2014). In semi-arid croplands of Spain, Boix-Fayos et al. (2009) estimated an average ER_{SOC} at sub-catchment scale (8–125 ha) of 0.59 ± 0.43. In this study, we hypothesized that the ER_{SOC} of different SOC pools, such as those of the unprotected and physically, chemically and biochemically protected SOC, are influenced by the presence or absence, and by the type, of temporary CC in an olive orchard. To test this hypothesis, we selected six runoff plots managed with three management practices: I) Conventional tillage (chisel plough passes and vegetation control), II) a mixture of plant species as CC and III) a uniform CC with one species. Sediment yield was recorded, and soil and sediment samples were collected and analysed for different SOC fractions during one hydrological year under several types of rainfall events.

2. Material and methods

2.1. Study area

The 'Santa Marta' commercial olive orchard was the site of this study. This orchard is located in SW Spain (37° 20′ 36″ N; 6° 13′ 45″W), in the province of Seville, near Benacazón village, at an average elevation of 92 m above sea level (Fig. 1a). The olive plantation was established in 1985 with trees planted at 8 × 6 m (more details in Gómez et al., 2009). The olive variety, Gordal, used as a table olive, is common in the area. Runoff plot experiments have been performed in this farm since 2003. Six bounded runoff plots (RP) were established between 2003 and 2005. Each RP (480 m^2) is 8 m wide (between 2 tree lines) and 60 m long, laid out with the longest dimension parallel to the maximum slope and to the tree lines (Fig. 1b, c). The slope is uniform, oriented in the north-west direction with an average slope gradient of 14.9 %, 15.6 %, 14.5 %, 13.0 %, 12.2 % and 12.8 % in RP1, RP2, RP3, RP4, RP5 and RP6, respectively.

Differential inter-row soil management started in the area the season before the delimitation of the RPs (Fig. 1e). Two plots (RP2 and RP4)

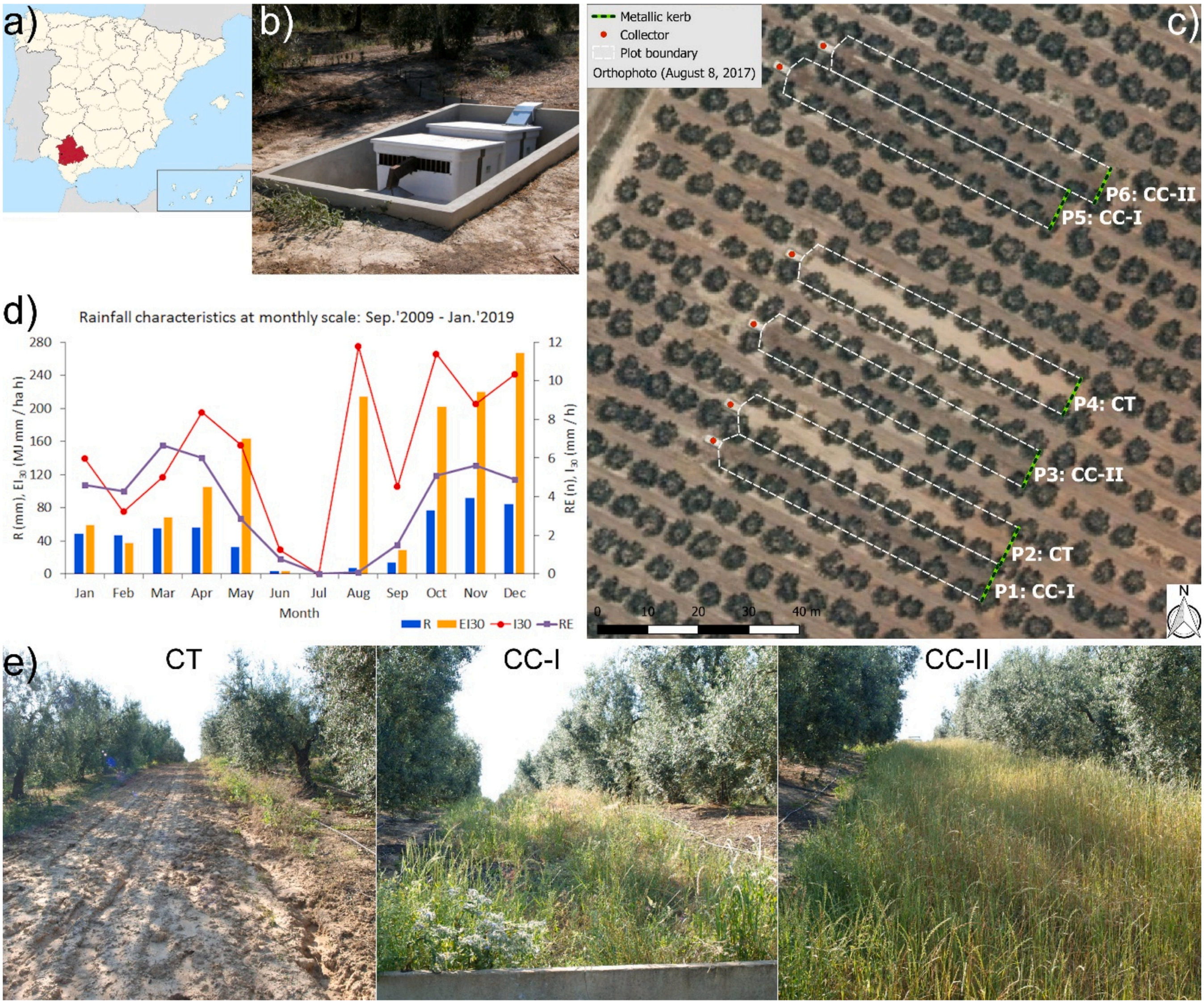

Fig. 1. Location of the study area (black dot) in Seville province (in red), SW Spain (a); picture of the overland flow collectors (b); aerial photo of the farm, showing the extension of the six plots (c); 10-yr average characteristic monthly values of the rainfall depth (R), erosivity (EI_{30}), intensity (I_{30}), and events (RE) (d); and pictures of the plots under the different soil and cover crop treatments at the end of May 2011 (e).

were devoted to conventional tillage (hereafter CT) consisted of regular chisel plough passes, 2–3 times a year normally during winter and spring at 10–15 cm depth depending on ground vegetation growth. During the year described in this manuscript, the tillage dates were December 3rd 2010, April 18th 2011 and July 12th 2011. Another set of two plots (RP1 and RP5) consisted in a mixture of different selected plant species as cover crop (CC-I) of *Borago officinalis* L., *Daucus carota* L., *Echium plantagineum* L., *Foeniculum vulgare* Mill, *Hedysarum coronarium* L., *Matricaria chamomilla* L., *Melilotus officinalis* L., *Moricandia moricandioides* Boiss., *Cichorium intybus* L., *Fagopyrum esculentum* Moench. and *Taraxacum officinale*. These plants were manually sown during early fall at 15 kg of seed per ha in the area outside the vertical olive canopy projection, which is in the range of recommended dose for farmers to balance cost and effectiveness of implementation. The third set of two plots (RP3 and RP6) was a uniform CC (CC-II) of *Lolium multiflorum* Lam. sown at 80 kg of seeds per ha in fall of 2009 and 2010. In both sets, the CC area was 4-m width. The maintenance of the CC includes mechanical (for CC-I) or chemical (for CC-II) removal of the cover and a permanent bare soil strip under the tree line maintained with herbicides. The intercrop strip was fertilized at the time of seeding with calcium ammonium nitrate 27 (13.5 ammonium N and 13.5 nitric N) equivalent to 40 FU of N, by direct application on the soil in the CC plots. In the two CC-I plots, plants were mechanically mowed in May, although if rains were abundant, additional passes were carried out in the previous months, whereas plants of the two CC-II plots were chemically killed in late winter or early spring, depending on the previous total rainfall depth. Olive trees were ferti-irrigated with ammonium sulfate in February (1.6 kg $tree^{-1}$) and from April to October, during the irrigation season. The amount of water applied during the drip irrigation season was, on average, 240 mm, although it varied slightly from year to year depending on the rainfall conditions.

The soil is a well-drained Petrocalcic Palexeralf (Soil Survey Staff, 2014), with an average organic matter, clay, silt and sand contents for the top 20 cm of 1.6 %, 16.6 %, 36.7 % and 46.6 %, respectively, and a texture class ranging from loamy sand to loam. In previous studies, Guzmán et al. (2010, 2019b) determined the main soil properties (Table 1). Bulk density ranges between 1.44 and 1.68 g cm^{-3}, and macroaggregate stability ranges between 0.152 and 0.286 kg kg^{-1} (Guzmán et al., 2019b). There is no presence of rills below the tree lines, and rills (ca. 5 cm of maximum depth) only appear along the inter-row land after the intense rainfall events in the CT plots.

The climate is subtropical semi-humid Mediterranean with an

Table 1
Average values and standard deviation (in brackets) of soil properties at the plots under different managements (CT and CC) and soil depth (0–10 and 10–20 cm depth) of the inter-canopy area (data source: Guzmán et al., 2010, 2019b). Soil sampling was carried out previously to the experimental setup.

Management	Soil depth (cm)	BD ($Mg\ m^{-3}$)	Sand (%)	Silt (%)	Clay (%)	Texture	MAE (kg/kg)
CT	0–10	1.44 (0.08)	53.1 (16.8)	31.8 (14.4)	15.1 (18.9)	Sandy loam	0.152 (0.103)
	10–20	1.56 (0.08)	46.5 (17.5)	37.4 (13.7)	16.1 (3.8)	Sandy loam	0.286 (0.091)
CC	0–10	1.68 (0.28)	50.6 (12.9)	34.0 (10.0)	15.4 (2.9)	Loam	0.232 (0.070)
	10–20	1.46 (0.08)	36.3 (8.2)	43.6 (10.5)	20.1 (2.2)	Loam	0.278 (0.046)

BD: Bulk density; MAE: Macroaggregate stability.

average annual precipitation of 519 mm (between September 2009 and August 2019), concentrated mostly in late fall and winter, and presents a strong inter-annual variability (e.g., 257 mm in 2017/2018, and 987 mm in 2009/10). The average annual air temperature was of 18.6 °C. Based on a 10-year record (2009–2019) of rainfall parameters, three moisture periods can be distinguished: I) the dry season (DS), from June to September (4 months; 0.6 rainfall events per month on average), with an average rainfall depth ($\overline{R}$), maximum intensity ($\overline{I_{30}}$) and rainfall erosivity ($\overline{EI_{30}}$) of 6.2 mm month^{-1}, 4.4 mm h^{-1} and 61.8 MJ mm ha^{-1} h^{-1}, respectively; II) the heavy-rainy season (HRS), from October to December (3 months; 5.2 events per month; $\overline{R} = 84.7$ mm month^{-1}; $\overline{I_{30}} = 10.2$ mm h^{-1}; $\overline{EI_{30}} = 229.7$ MJ mm ha^{-1} h^{-1}); and III) the rainy season (RS) from January to May (5 months; 4.9 events per month; $\overline{R} = 48.0$ mm month^{-1}; $\overline{I_{30}} = 5.9$ mm h^{-1}; $\overline{EI_{30}} = 86.8$ MJ mm ha^{-1} h^{-1}) (Fig. 1d). Rainfall erosivity, EI_{30}, was calculated at monthly scale as the sum of the rainfall erosivities at event scale; based on the approach of McGregor and Mutchler (1976) to assess the kinetic energy. This energy-intensity equation is currently recommended by the RUSLE and RUSLE2 soil erosion model development teams (Nearing et al., 2017). In previous studies performed in the same plots, higher values of runoff yield and soil erosion were recorded under CT treatment (19.4 Mg ha^{-1} year^{-1} on average) whereas CC triggered higher spatial and temporal stability of runoff and runon, and lower values of soil erosion (0.4 Mg ha^{-1} year^{-1}) (Gómez et al., 2009; López-Vicente et al., 2016).

2.2. Test period, and soil and sediment sampling

In the hydrological year 2010-2011 (October 2010 to September 2011), six years after establishing the CT and CC-II treatments (CT, CC-I) and the second of CC-I, runoff and sediment yield collection was performed using a system of three fiberglass collection tanks with flow splitters (ratio 1:15), allowing measurement of up to 110 m^3 equivalent to 230 mm of runoff. Once carefully levelled, the splitters were kept free of leaves, small branches and other organic residues with a small protection net located upstream. The experiment site was completed with an automatic weather station (more details about the field installation in Gómez et al., 2009). During the test period, twelve field surveys were carried out and 12 time-integrated sediment samples were collected at each collector. The interval between each survey was different and depended on the frequency and intensity of the rainfall events. The time-integrated period (TIP) was defined as the interval between each field survey. The number of accumulated rainfall events was different among the TIPs, averaged 4.3 with a minimum and maximum of 1 and 11 events. Soil samples were collected at two depths (0–5 and 5–15 cm) and four replications were taken at each soil depth in the CC and CT plots in May 2010.

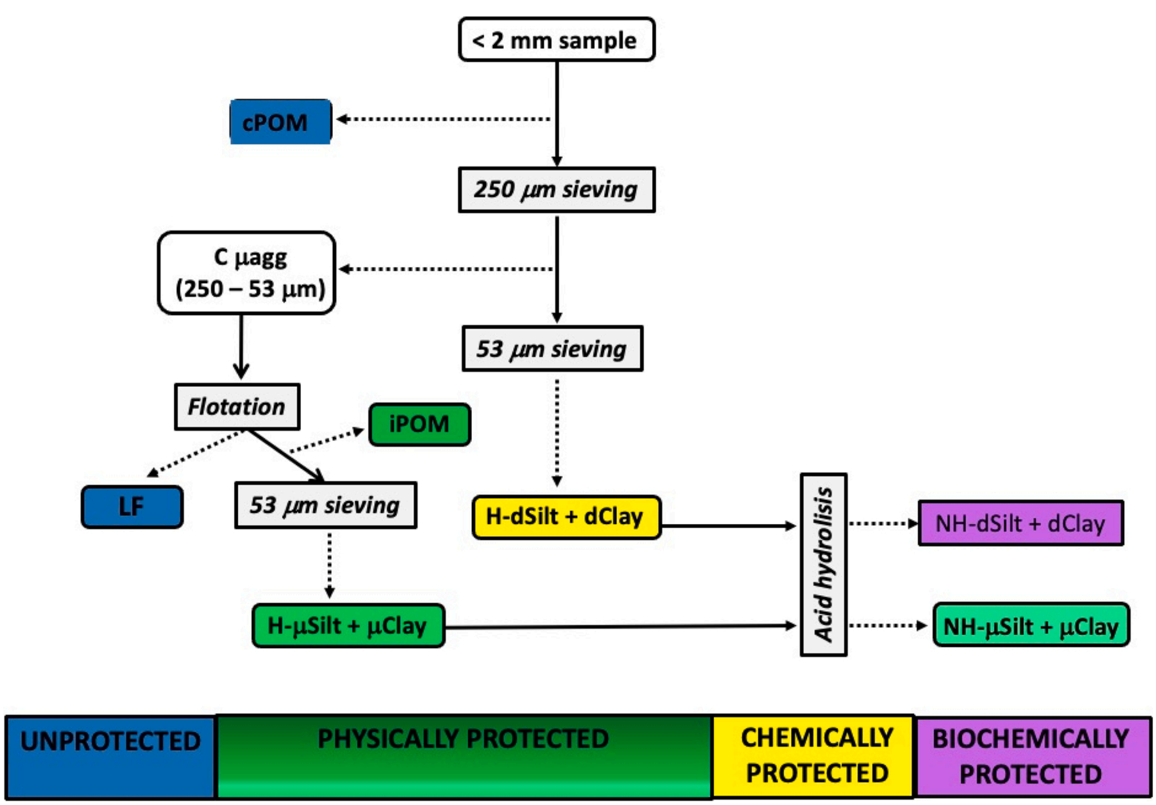

Fig. 2. Fractionation scheme to isolate and quantify the unprotected, and physically, chemically and biochemically protected SOC fractions.

2.3. Soil carbon fractionation

Separation of the various soil C pools of the soil and sediment samples was accomplished by a combination of physical and chemical fractionation techniques in a simple, three-step process modified from Stewart et al. (2009) (Fig. 2), using 50 g for each soil and sediment sample analyzed. For sediment, samples from each collectors and events were subjected to soil organic carbon fractionation. However, soil organic carbon fractionation was not possible when not enough material was collected in the collector. This was the case for the CC plots on 2nd December, 27th April and 10th May TIPs. The method can described briefly like this: after a first step consisting in the partial dispersion and physical fractionation of the soil in wet conditions to obtain three size fractions (>250 μm, 53–250 μm, and <53 μm), a second step, which involved further fractionation of the 53–250 μm fraction previously isolated, followed. The >250 μm, 53–250 μm, and <53 μm fractions isolated after the first step corresponded to the coarse non-protected particulate organic matter (cPOM), microaggregated (μagg), and easily dispersed silt and clay (dSilt + dClay) fractions, respectively. In this second step, a density flotation with sodium chloride was used to isolate the fine non-protected particulate organic matter (LF) from the microaggregated fraction. After removing LF, the heavy fraction was dispersed overnight by shaking with 15 glass beads and passes through a 53 μm sieve, separating the microaggregated protected POM (> 53 μm in size, iPOM) from the microaggregated derived silt- plus clay-size fractions (μSilt + μClay). The third step involved the acid hydrolysis of each of the isolated silt- plus clay-sized fractions. The silt- plus clay-size fractions from both the density flotation (μSilt + μClay) and the initial dispersion and physical fractionation (dSilt + dClay) were subjected to acid hydrolysis as described by Plante et al. (2006). Acid hydrolysis consisted of incubating the samples at 95 °C for 16 h in 25 ml of 6 M HCl. After hydrolysis, the suspension was filtered and washed with deionized water over a glass-fibre filter. Residues were oven-dried at 60 °C and weighed. These fractions represent the non-hydrolysable C fractions (NH-dSilt + dClay, and NH-μSilt + μClay). The hydrolysable C fractions (H-dSilt + dClay, and H-μSilt + μClay) were determined by difference between the total organic C content of the fractions and the C content of the non-hydrolysable fractions.

This three-step process isolated a total of seven fractions, and it is based on the assumed link between the isolated fractions and the protection mechanisms involved in the stabilization of organic C (Six et al., 2002). The unprotected pool included the cPOM and LF fractions, isolated in the first and second fractionation steps, respectively. The physically protected SOC consisted of the SOC measured in the microaggregates. It included not only the iPOM but also the hydrolysable (H-μSilt + μClay) and non-hydrolysable (NH-μSilt + μClay) SOC of the intermediate fraction (53–250 μm). The chemically and biochemically protected pools correspond to that hydrolysable (H-dSilt + dClay) and non-hydrolysable (NH-dSilt + dClay) SOC in the fine fraction (< 53 μm), respectively. Total SOC and C_{org} of each of the soil fractions were determined after digesting the soil and sediment samples, previously grounded with a ball mill, with dichromate and sulphuric acid following the method proposed by Anderson and Ingram (1993).

2.4. Assessment of the SOC enrichment ratios

The sediment/soil enrichment ratios for the total (ER_{SOC}), the non-protected ($ER_{N\text{-}POC}$) and the protected (ER_{POC}) organic carbon stocks were calculated, taking into account the organic carbon content of these fractions in the top 5 cm of soil of the plots and in the sediment collected from these plots, and the contribution of the sediment yield of each of the 12 TIPs to the total. The differences of the $ER_{N\text{-}POC}$ and ER_{POC} values in the CC and CT plots were analysed over the three moisture seasons.

2.5. Statistical analysis

The analysis of variance (ANOVA; one-way) of: (I) the sediment yield, (II) the total and SOC fractions contents in the soil samples collected in the different runoff plots at two soil depth intervals; (III) the total and SOC fractions contents in the sediment samples from the six collectors; and (IV) the ER_{SOC}, $ER_{N\text{-}POC}$ and ER_{POC} in the different plots was performed using SigmaPlot software (version 13.0) and the Shapiro-Wilk Normality Test at *P-value* < 0.05.

3. Results

3.1. Erosive events and sediment yield

A total number of 52 rainfall events were registered during the test period, adding up to 715 mm of precipitation. These events had an average rainfall intensity and mean and total erosivity of 9.2 mm h^{-1}, 47 MJ mm ha^{-1} h^{-1} $event^{-1}$ and 2440 MJ mm ha^{-1} h^{-1} yr^{-1}, respectively. Despite that 74 % of the rainfall depth was registered between October and March, the most erosive event (I_{30} = 77 mm h^{-1}) took place in May 2011, reaching 1108 MJ mm ha^{-1} h^{-1} $event^{-1}$. No rainfall event was observed in June, July and August 2011. The rainfall characteristics of each TIP are shown in Table 2. Twenty-eight rainfall events took place during the HRS (October to December), with a mean rainfall depth ($\overline{R}$), maximum intensity ($\overline{I_{30}}$) and erosivity ($\overline{EI_{30}}$) –per event– of 13.6 mm, 8.7 mm h^{-1} and 36.1 MJ mm ha^{-1} h^{-1}, respectively. During the five months of the RS (January to May), twenty-two rainfall events were observed, with similar values of $\overline{R}$ (13.5 mm) and $\overline{I_{30}}$ (9.7 mm h^{-1}) but almost double of $\overline{EI_{30}}$ (60.7 MJ mm ha^{-1} h^{-1}) than HRS. These values were mainly explained by the intense rainfall event that took place on May 19, 2011 that reached a rainfall depth of 52.5 mm. This event explained 45 % of the total annual rainfall erosivity. During the DS (June to September), we only observed two rainfall events, with values of $\overline{R}$, $\overline{I_{30}}$ and $\overline{EI_{30}}$ of 19.8 mm, 10.0 mm h^{-1} and 46.2 MJ mm ha^{-1} h^{-1}, respectively.

During the test period, the sediment yield (SY) in the two plots under CT was the highest ($\overline{SY}$ = 1.72 Mg ha^{-1} TIP^{-1}) whereas the SY in the CC-I ($\overline{SY}$ = 0.83 Mg ha^{-1} TIP^{-1}) and CC-II ($\overline{SY}$ = 0.70 Mg ha^{-1} TIP^{-1}) plots was lower than half. Differences of SY between CC-I and CC-II plots were not significant (P = 0.723 per TIP and P = 0.795 per event), and therefore, these plots will be considered as replicate hereafter. As expected, the differences in SY per TIP between CT and CC were significant (P = 0.019) (Fig. 3a).

Taking into account that every TIP is a unique combination of different rainfall events, the mean SY per event was estimated for the 12 TIPs (Table 3; Fig. 3b). The highest rates were obtained in December 2010 (TIP #4, 5 and 6; between 0.49 and 1.17 Mg ha^{-1} $event^{-1}$, on average in the six plots) and May 2011 (0.39 Mg ha^{-1} $event^{-1}$). During the intense event of May 2011, $\overline{SY}$ in the CC plots was only of 0.33 Mg ha^{-1} $event^{-1}$ –owing to the protecting role of the vegetation– and in the CT plots of 0.52 Mg ha^{-1} $event^{-1}$. Over the three rainfall regimes, the rates of SY changed in the six plots with the highest values in HRS ($\overline{SY}$ = 1.70 Mg ha^{-1} TIP^{-1} and 0.46 Mg ha^{-1} $event^{-1}$), and with moderate and low values in RS ($\overline{SY}$ = 0.56 Mg ha^{-1} TIP^{-1} and 0.160 Mg ha^{-1} $event^{-1}$) and DS ($\overline{SY}$ = 0.02 Mg ha^{-1} TIP^{-1} and 0.012 Mg ha^{-1} $event^{-1}$). The differences in the values of SY per event between the CC and CT plots were statistically significant (P = 0.029), and clear differences appeared between the mean values of the CC ($\overline{SY}$ = 0.22 Mg ha^{-1} $event^{-1}$) and CT ($\overline{SY}$ = 0.46 Mg ha^{-1} $event^{-1}$) plots. This pattern was constant over time and the values of SY followed this sequence: HRS and CT ($\overline{SY}$ = 0.69 Mg ha^{-1} $event^{-1}$) > HRS and CC ($\overline{SY}$ = 0.35 Mg ha^{-1} $event^{-1}$) > RS and CT ($\overline{SY}$ = 0.27 Mg ha^{-1} $event^{-1}$) > RS and CC ($\overline{SY}$ = 0.10 Mg ha^{-1} $event^{-1}$) > DS and CT ($\overline{SY}$ = 0.02 Mg ha^{-1} $event^{-1}$) > DS and CC ($\overline{SY}$ = 0.01 Mg ha^{-1} $event^{-1}$).

Table 2
Rainfall characteristics during the different time-integrated periods (TIP) along the test period (hydrological year 2010-2011).

Survey		Regime	*RE*	*ΣR*	$\overline{R}$	$\overline{I_{30}}$	$\overline{D}$	*ΣEI₃₀*	$\overline{EI_{30}}$
Date	#	(type)	(n)	(mm)	(mm)	(mm/h)	(s)	(MJ mm / ha h TIP)	(MJ mm / ha h event)
14/Oct/2010	S1	HRS	4	54.5	13.6	7.5	6,739	68.65	17.16
05/Nov/2010	S2	HRS	1	16.0	16.0	32.0	1,800	144.12	144.12
02/Dec/2010	S3	HRS	11	96.0	8.7	4.5	7,833	54.26	4.93
14/Dec/2010	S4	HRS	5	75.0	15.0	10.0	4,977	216.99	43.40
28/Dec/2010	S5	HRS	3	93.5	31.2	14.7	8,029	422.43	140.81
13/Jan/2011*	S6	HRS	4	44.5	11.1	9.5	3,893	105.59	26.40
23/Feb/2011	S7	RS	5	59.5	11.9	8.6	5,245	69.41	13.88
16/Mar/2011	S8	RS	5	88.5	17.7	7.8	10,566	81.53	16.31
27/Apr/2011	S9	RS	6	40.5	6.8	3.2	6,025	19.61	3.27
10/May/2011	S10	RS	5	55.0	11.0	7.2	5,216	57.64	11.53
24/May/2011	S11	RS	1	52.5	52.5	77.0	2,455	1,107.69	1,107.69
15/Sep/2011	S12	DS	2	39.5	19.8	10.0	5,456	92.47	46.23

RE: rainfall events, *ΣR*: accumulated rainfall, $\overline{R}$: average rainfall depth, $\overline{I_{30}}$: average maximum rainfall intensity, $\overline{D}$: mean duration, *ΣEI₃₀*: accumulated rainfall erosivity, $\overline{EI_{30}}$: average rainfall erosivity; DS: dry season, RS: rainy season, and HRS: heavy rainy season. *: The most erosive rainfall event during this TIP took place in December, during the HRS.

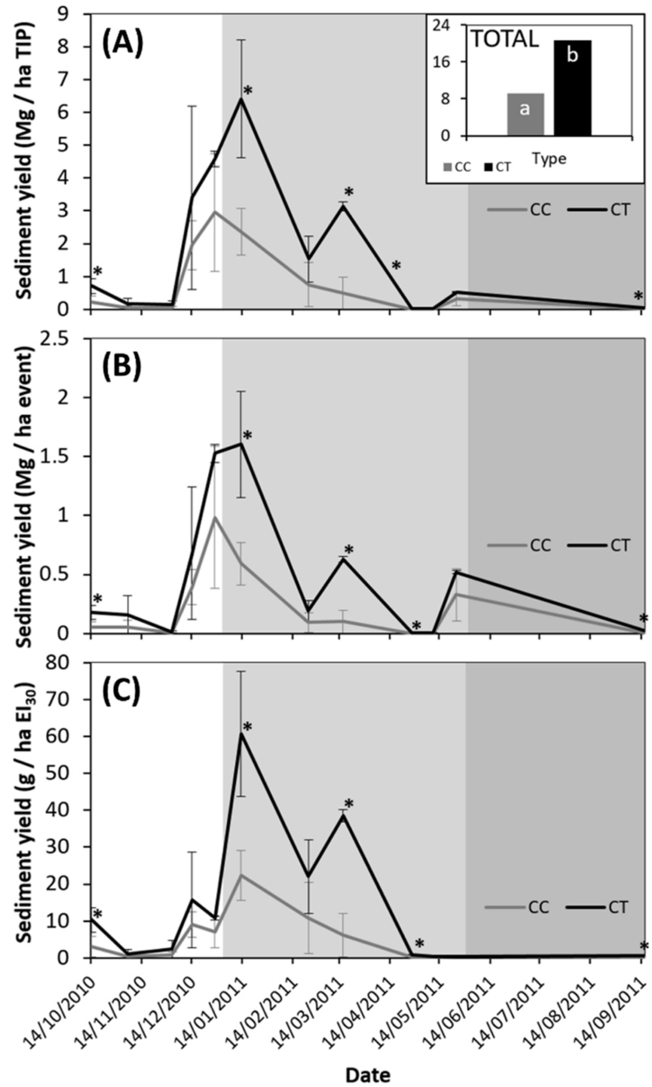

Fig. 3. Mean, standard deviation and total values (inset figure) of sediment yield per time-integrated period (A), rainfall event (B) and rainfall erosivity (C) in the cover crop (CC) and conventional tillage (CT) plots. The white, light grey and dark grey areas correspond to the heavy-rainy (HRS), rainy (RS) and dry (DS) seasons. The asterisks and different lowercase letters in the inset figures indicate significant differences between the CC and CT plots at 0.05 level in the corresponding date.

As the rainy seasons along the hydrological year had distinct values of rainfall depth, intensity and erosivity, the mean SY per rainfall erosivity unit (EI_{30}) was calculated (Table 4) (Fig. 3c). The highest values of SY-EI_{30} appeared between December and March, with mean values in the six plots that ranged between 8.3 and 35.2 g ha^{-1} EI_{30}^{-1}, whereas SY remained below 0.5 g ha^{-1} EI_{30}^{-1} between April and September. Thus, the effective erosivity of the intense rainfall event that took place in May 2011 was much lower than the erosivity associated to the events that happened in fall and winter. The mean SY during the HRS, RS and DS was of 10.3, 6.5 and 0.3 g ha^{-1} EI_{30}^{-1}, respectively. The effective erosivity in the CT plots ($\overline{SY}$ =13.7 g ha^{-1} EI_{30}^{-1}) was on average 172 % higher than in the CC plots ($\overline{SY}$ =5.0 g ha^{-1} EI_{30}^{-1}), and the difference was statistically significant ($P = 0.007$).

3.2. Protected and non-protected SOC content in the soil samples

Before fractionation, the highest SOC content in the top 5 cm soil was found in the CC plots (14.6 ± 4.0 mg C_{org} g^{-1} soil) whereas in the CT plots the content (9.3 ± 0.9 mg C_{org} g^{-1} soil) was significantly lower ($P = 0.021$). On average –from all the plots, the SOC in the 5−15 cm soil depth was 19 % lower than in the 0−5 cm soil. In particular, the SOC in the 5−15 cm soil depth of the CC plots (11.0 ± 3.6 mg C_{org} g^{-1} soil) was only 7% higher than that in the CT plots (10.3 ± 2.6 mg C_{org} g^{-1} soil) and differences among treatments were not significant ($P = 0.722$) at this soil layer. The SOC in the soil particles of 250–2000 μm, 53–250 μm and <53 μm of the top 5 cm soil of the CC plots were, on average, 1.8, 1.4 and 1.1 times higher than that of the soil under CT treatment. In the 5−15 cm soil depth, and following the overall pattern described above, the SOC in the different soil particles sizes in the CC plots were similar to the content in the CT plots. When the analysis was focused on the SOC densities (e.g. mg C_{org} g^{-1} soil particle fraction) of the top 5 cm soil, the values in the CC plots were 1.2, 1.4 and 1.5 times higher than those in the CT plots in the 250–2000 μm, 53–250 μm and <53 μm fractions, respectively. Differences in SOC density between CC and CT plots decreased in the 5−15 cm soil layer and were not significant in any case: P = 0.652, 0.070 and 0.435 in the 250–2000 μm, 53–250 μm and <53 μm fractions.

The cPOM (1.8 times) and LF (2.7 times) fractions, and thus unprotected top 5 cm soil SOC (1.9 times) were significantly higher in the CC than in the CT plots (Table 5). The LF fraction in the 5−15 cm soil layer was also significantly higher in the CC although it was not the case for the total unprotected SOC. Total protected C, and particularly the biochemically-physically-chemically fraction, were significantly higher in CC plots for the top 5 cm of soil. However, this was not true for the 5−15 cm soil layer. Unprotected SOC accounted for a mean of 59.6 % of the total SOC in the top 5 cm of soils in the CC plots whereas figure

Table 3
Sediment yield measured during each time-integrated period (TIP), and estimated at rainfall event scale, for the CC and CT plots. The same lowercase letter in the mean sediment yield per TIP and event during the whole hydrological cycle indicates that no significant difference was observed at 0.05 level between the six plots.

Survey	Sediment yield (Mg / ha TIP)						Sediment yield (Mg / ha event)					
#	RP1 CC-I	RP2 CT	RP3 CC-II	RP4 CT	RP5 CC-I	RP6 CC-II	RP1 CC-I	RP2 CT	RP3 CC-II	RP4 CT	RP5 CC-I	RP6 CC-II
S1	0.498	0.873	0.135	0.550	0.105	0.096	0.124	0.218	0.034	0.137	0.026	0.024
S2	0.137	0.274	0.051	0.043	0.032	0.004	0.137	0.274	0.051	0.043	0.032	0.004
S3	0.118	0.223	0.011	0.043	0.033	0.003	0.011	0.020	0.001	0.004	0.003	<0.001
S4	2.892	1.425	2.226	5.380	1.357	1.347	0.578	0.285	0.445	1.076	0.271	0.269
S5	4.984	4.418	3.843	4.740	0.972	2.023	1.661	1.473	1.281	1.580	0.324	0.674
S6	2.877	7.678	2.897	5.141	1.391	2.286	0.719	1.919	0.724	1.285	0.348	0.571
S7	1.762	2.022	0.435	1.038	0.441	0.373	0.220	0.253	0.054	0.130	0.055	0.047
S8	1.205	3.230	0.369	3.047	0.238	0.175	0.241	0.646	0.074	0.609	0.048	0.035
S9	0.006	0.019	0.004	0.016	0.001	0.002	0.001	0.003	0.001	0.003	<0.001	<0.001
S10	0.012	0.008	0.004	0.037	0.004	0.003	0.002	0.002	0.001	0.007	0.001	0.001
S11	0.186	0.531	0.509	0.509	0.530	0.090	0.186	0.531	0.509	0.509	0.530	0.090
S12	0.022	0.029	0.012	0.069	0.005	0.007	0.011	0.015	0.006	0.034	0.002	0.004
Total	14.699	20.730	10.498	20.611	5.108	6.409	3.893	5.638	3.181	5.418	1.640	1.720
Mean	1.225a	1.727a	0.875a	1.718a	0.426a	0.534a	0.324a	0.470a	0.265a	0.451a	0.137a	0.143a

Table 4
Calculated sediment yield per rainfall erosivity unit (EI_{30}) during each time-integrated period (TIP). The same lowercase letter in the mean sediment yield per EI_{30} during the whole hydrological cycle indicates that no significant difference was observed at 0.05 level between the six plots.

Survey	Sediment yield (g / ha EI_{30})					
#	RP1 (CC-I)	RP2 (CT)	RP3 (CC-II)	RP4 (CT)	RP5 (CC-I)	RP6 (CC-II)
S1	7.2	12.7	2.0	8.0	1.5	1.4
S2	1.0	1.9	0.4	0.3	0.2	<0.1
S3	2.2	4.1	0.2	0.8	0.6	<0.1
S4	13.3	6.6	10.3	24.8	6.3	6.2
S5	11.8	10.5	9.1	11.2	2.3	4.8
S6	27.2	72.7	27.4	48.7	13.2	21.6
S7	25.4	29.1	6.3	15.0	6.4	5.4
S8	14.8	39.6	4.5	37.4	2.9	2.1
S9	0.3	1.0	0.2	0.8	0.1	0.1
S10	0.2	0.1	0.1	0.6	0.1	<0.1
S11	0.2	0.5	0.5	0.5	0.5	0.1
S12	0.2	0.3	0.1	0.7	<0.1	0.1
Total	103.8	179.1	61.0	148.8	34.0	41.9
Mean	8.7a	14.9a	5.1a	12.4a	2.8a	3.5a

(mean of 40.6 %) was significantly lower in the CT plots. The contribution of the protected SOC to the total SOC in the top 5 cm of soils of the CT plots (mean of 59.3 %) was significantly higher than that of the CT plots (40.3 %).

3.3. Loss of protected and non-protected organic carbon

The average loss of total SOC during the whole test-period was of 148.4 and 221.5 kg C_{org} ha^{-1} yr^{-1} in the CC and CT plots, respectively, but the difference between both values was not significant ($P = 0.156$). However, when the statistical analysis was done at TIP scale, the differences in the losses of total SOC among treatments were significant ($P = 0.029$). Regarding the distinct fractions, the total loss of non-protected C_{org} averaged 51.2 and 56.9 kg C_{org} yr^{-1} in the CC and CT plots without being statistically significant ($P = 0.813$) (Fig. 4). The mean total loss of protected C_{org} for CC plots was 97.0 kg C_{org} yr^{-1}, which was significantly lower ($P = 0.042$) than the 163.4 kg C_{org} yr^{-1} recorded in the CT plots (Fig. 4).

The highest proportion of organic carbon which was eroded corresponded to the physically protected carbon (53–250 μm) and averaged during the studied hydrological period 45 % and 44 % of the total in CT and CC, respectively, whereas the lowest was the chemically (13 %) and biochemically protected (10 %) in the CT and CC, respectively. These results were in agreement with the higher content of sand sized particles in the soil of both the CC and CT plots.

Overall, the loss of protected SOC in the sediment of the CT plots reached up to 74 % of the total SOC loss, whereas this percentage was, on average, of 65 % in the CC plots. This pattern was especially marked in the loss of the bio-chemically protected fraction, which was 1.72 times higher in the CT plots than in the CC plots. Despite the distinct behaviour of the CC and CT plots, the differences at TIP scale between the non-protected ($P = 0.518$), physically protected ($P = 0.774$), chemically protected ($P = 0.721$), bio-chemically protected ($P = 0.133$) and total protected ($P = 0.553$) fractions of the two treatments were not statistically significant (Fig. 4). However, when the differences were analysed at annual scale –accumulated loss of SOC per plot– the differences became significant between the total protected ($P = 0.042$) and bio-chemically protected ($P = 0.013$) fractions of the two treatments.

The mean C_{org} content of the total eroded sediment was of 17.1 and 10.7 mg C_{org} g_{sed}^{-1} in the CC and CT plots, respectively. Figures for the non-protected and physically, chemically, bio-chemically and total protected fractions were of 5.5, 7.7, 2.2, 1.7 and 11.6 mg C_{org} g_{sed}^{-1} in the CC plots, whereas values were of 2.8 (26 %), 4.8 (45 %), 1.4 (13 %), 1.7 (16 %) and 8.0 (74 %) mg C_{org} g_{sed}^{-1} in the CT plots.

During the 12 TIPs, the evolution in the loss of the protected and non-protected SOC fractions was different between the CC and CT plots. The

Table 5
Mean and standard deviation content of the non-protected and protected fractions of SOC in the 5 soil samples collected in CC and CT plots at two soil depth intervals. Different lowercase letters in the same column and within the same soil depth range indicates the difference was significant at 0.05 level.

Depth		Non-protected (mg C_{org} / g soil)			Protected (mg C_{org} / g soil)					
(cm)		>250 μm	53–250 μm	Total	53–250 μm			<53 μm		Total
		cPOM	LF		Phy iPOM	Phy-Chem H-μSilt + μClay	Bio-Phy-Chem NH-μSilt + μClay	Chem H-dSilt + dClay	Bio-Chem NH-dSilt + dClay	
0–5	CC	4.79 ± 1.41a	1.78 ± 1.39a	6.37a	3.76 ± 0.90a	1.34 ± 0.59a	0.55 ± 0.24a	3.35 ± 0.63a	1.69 ± 0.57a	10.68a
0–5	CT	2.73 ± 0.68b	0.66 ± 0.27a	3.38b	2.70 ± 0.84a	0.95 ± 0.30a	0.27 ± 0.07b	3.12 ± 0.61a	1.27 ± 0.44a	8.31b
5–15	CC	2.12 ± 0.78a	1.50 ± 0.67a	3.62a	2.82 ± 1.02a	0.95 ± 0.34a	0.50 ± 0.22a	2.35 ± 0.96a	1.74 ± 0.74a	8.36a
5–15	CT	2.50 ± 0.65a	0.65 ± 0.26b	3.15a	1.68 ± 0.39a	1.22 ± 0.06a	0.37 ± 0.14a	3.38 ± 0.93a	1.08 ± 0.76a	7.73a

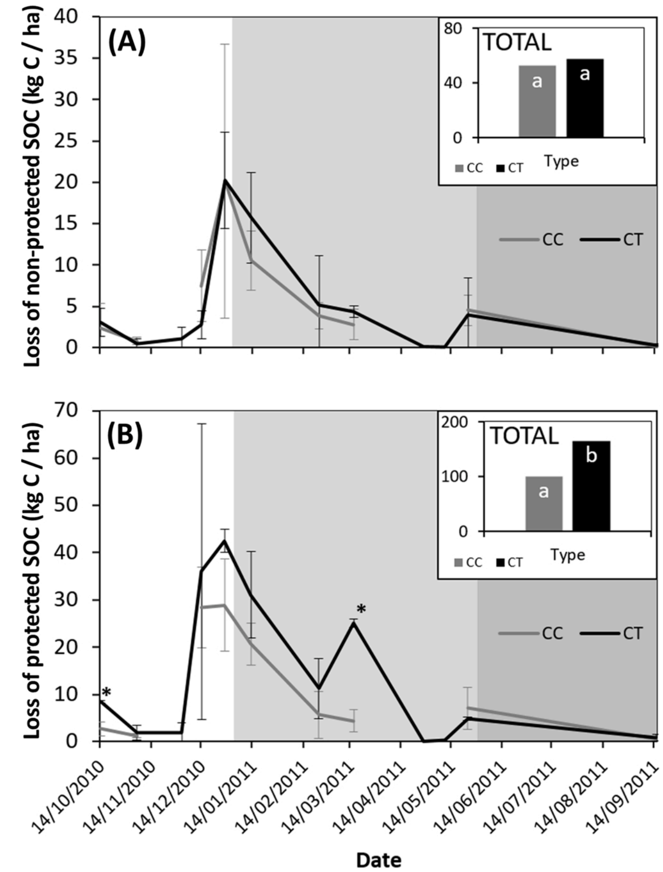

Fig. 4. Loss of non-protected (A) and protected (B) SOC during the 12 time-integrated periods and the whole hydrological cycle (inset) in the CC and CT plots. The white, light grey and dark grey areas correspond to the heavy-rainy (HRS), rainy (RS) and dry (DS) seasons. The asterisks and different lowercase letters indicate significant differences between the CC and CT plots at 0.05 level in the corresponding date.

highest rates of SOC loss were found in the TIP #4 (December), #5 (December) and #6 (January) in the CC plots, with an average rate of 38.7 kg C_{org} ha^{-1} TIP^{-1}; whereas the highest rates in the CT plots appeared in the TIP #4, #5, #6, #7 (February) and #8 (March), with an average rate of 38.8 kg C_{org} ha^{-1} TIP^{-1} (Fig. 5). During the remaining TIPs, the average rate of SOC loss was very low: 6.8 and 4.6 kg C_{org} ha^{-1} TIP^{-1}, in the CC and CT plots, respectively, and after excluding the TIPs when no SOC loss was observed. It is worth mentioning that only the collector of the plot #4 (CT) stored sediment during all TIPs. During the TIP #3, #9 and #10, no SOC loss was measured in the four plots with CC, highlighting the protecting role of the CC against soil erosion.

The loss of the physically protected fraction was the most important among the four fractions, in 70 % and 82 % of the TIPs in the CC and CT plots, respectively. In the CC plots, the bio-chemically protected fraction represented the lowest amount of SOC loss (ca. 10 %), whereas in the CT plots the loss of the bio-chemically protected fraction was on average 24 % higher than the loss of the chemically protected fraction (ca. 13 % of the total SOC loss). The non-protected fraction was the most important in 25 % and 9% of the TIPs in the CC and CT plots, respectively. During the three months of the heavy-rainy season (HRS), the average loss of total SOC was of 25.8 and 27.5 kg C ha^{-1} TIP^{-1} in the CC and CT plots, respectively. During the five months of the rainy season (RS), the average loss of total SOC was of 9.3 and 13.8 kg C ha^{-1} TIP^{-1} in the CC and CT plots, respectively, whereas during the four months of the dry season (DS), all rates were low and the average loss of total SOC was of 0.7 and 1.2 kg C ha^{-1} TIP^{-1} in the plots under CC and CT, respectively.

Based on the weight of the sediment, the highest concentrations of C_{org} appeared in the total protected fractions in the DS (25.8 and 18.0 mg C_{org} g^{-1} sediment in CC and CT) followed by the HRS and RS, with minor differences between the two latest rainfall seasons. Differences between the concentrations of the protected fractions of the CC and CT plots were not significant for the DS, HRS and RS (Table 6). However, the differences of the CC and CT plots between the DS and the other two rainfall regimes were significant. In particular, the physically protected fractions had the highest values both in the CC and CT plots compared with the other fractions and during the three rainfall seasons. The non-protected fractions presented lower values than those observed in the physically protected fractions and higher values than those obtained in the chemically and bio-chemically protected fractions. This pattern remained constant in the three rainfall regimes, either in the CC or in the CT plots, but no significant difference was obtained. The differences between the two treatments (CC *vs.* CT) were only significant in the physically protected fractions in the DS, and in the chemically protected fractions in the RS. More differences that are significant appeared when the analysis was done between the three rainfall regimes with the same treatment regarding the protected fractions. The chemically (between 1.0 and 7.5 mg C_{org} g^{-1} sediment) and bio-chemically (between 0.9 and 2.4 mg C_{org} g^{-1} sediment) protected fractions showed lower concentrations.

Taking into account the marked temporal changes in the rainfall depths and intensities in the study area over the year, we evaluated the relationship between the accumulated rainfall erosivity (ΣEI_{30}) between each field survey –called time-integrated period (TIP)– and the loss of the different SOC fractions in the different plots and treatments. In general, higher ΣEI_{30} values favoured an increasing loss of both total non-protected and total protected fractions, in particular during HRS (from October to December) when the soil surface cover presented its lowest values. The events recorded during RS (from January to May) –with the highest values of soil surface cover– and DS (from June to September) –almost no rainfall– triggered lower losses of SOC regardless the values of rainfall depth and/ or intensity.

3.4. Sediment carbon enrichment ratios of the protected and non-protected SOC fractions

On average, the calculated annual sediment/soil enrichment ratio for the total organic carbon (ER_{SOC}) was of 1.002 and 0.917 in the CC and CT plots, respectively (Table 7). In all fractions, except the bio-chemically (26 %) protected fractions, the ER_{SOC} in the CC plots tended to be greater than those values in the CT plots, although differences were not significant between the two treatments. The physically and bio-chemically protected fractions had $ER_{SOC} > 1$, whereas the other fractions presented $ER_{SOC} <1$, especially the chemically protected fractions that had the lowest ER_{SOC}, both in the CC ($\overline{ER_{SOC}} = 0.64$) and CT ($\overline{ER_{SOC}} = 0.45$) plots. However, none of the ER_{SOC} values were significantly different from 1.

Over the three soil moisture seasons, the highest ER_{SOC} of the total organic carbon appeared in the DS, both in the CC ($\overline{ER_{SOC}} = 1.99$) and CT ($\overline{ER_{SOC}} = 2.06$) plots. The lowest ratios were found in the RS ($\overline{ER_{SOC}} = 0.96$ in CC; $\overline{ER_{SOC}} = 0.90$ in CT) and HRS ($\overline{ER_{SOC}} = 0.95$ in CC; $\overline{ER_{SOC}} = 0.92$ in CT), without clear differences between these two rainfall regimes. This temporal pattern was repeated in all protected and non-protected fractions, but the ER_{SOC} in the non-protected fractions were lower than those of the total protected fractions (Fig. 6).

4. Discussion

4.1. Temporal patterns of sediment yield under contrasted soil management

Annual rainfall during the studied period was 38 % higher than the 25-year average, but within the wide range of variability which characterises the Mediterranean climate of the area. Overall, the temporal

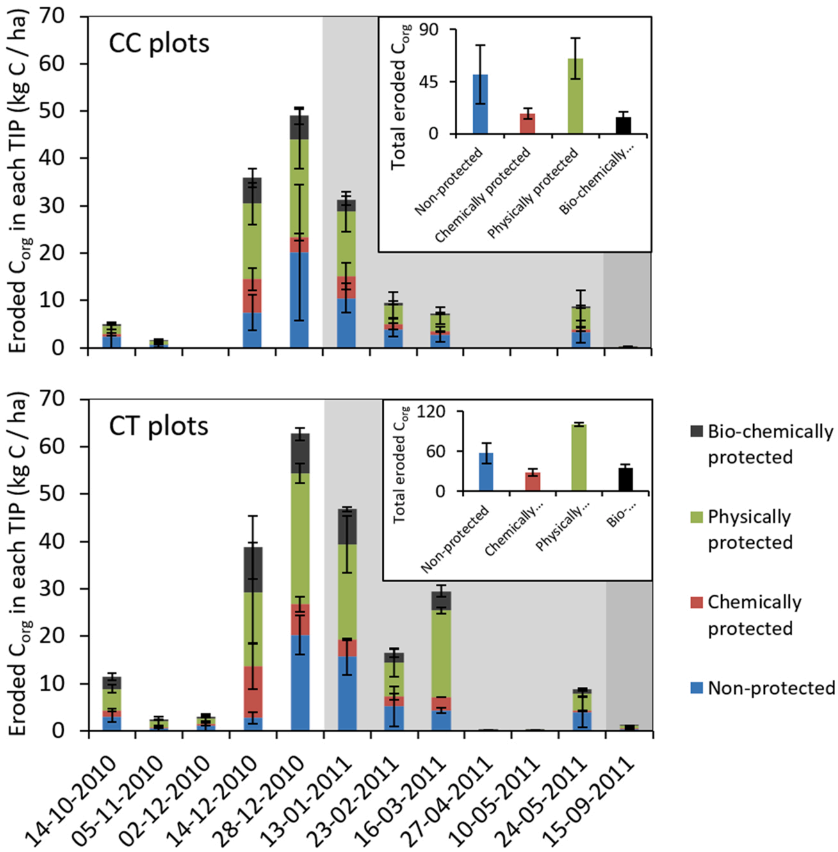

Fig. 5. Loss of the different (non-)protected SOC fractions during the 12 time-integrated periods and the whole hydrological cycle (inset) in the CC and CT plots. The physically protected stock in these charts included the previous physically protected (as defined in the Section 2.3. Soil carbon fractionation), the physically-chemically protected, and the bio-physically-chemically protected fractions. The white, light grey and dark grey areas correspond to the heavy-rainy (HRS), rainy (RS) and dry (DS) seasons.

Table 6
Weighted mean, and standard error of the mean, content of the non-protected and protected C_{org} fractions in the sediment samples collected from the CC and CT plots during the three soil moisture regimes: HRS, RS and DS. Different lowercase letters in the same column indicates the difference was significant at 0.05 level.

Moisture regime		Contents of organic carbon in the sediment (mg C_{org}/g sediment)				
		Non-protected*	Protected			
			Physically**	Chemically†	Bio-Chemically††	Total
HRS	CC	5.46 ± 0.83a‡,a‡‡	7.02 ± 1.26a‡, a‡‡	2.05 ± 0.43a‡, b‡‡	1.75 ± 0.29a‡, b‡‡	10.83 ± 1.88a‡, a‡‡
	CT	2.81 ± 0.55a‡, a‡‡	4.57 ± 0.05a‡, a‡‡	1.49 ± 0.34a‡, a‡‡	1.85 ± 0.18a‡, a‡‡	7.91 ± 0.47a‡, a‡‡
RS	CC	6.47 ± 1.09a‡, a‡‡	7.57 ± 1.71a‡, a‡‡	1.46 ± 0.09a‡, a‡‡	0.87 ± 0.14a‡, a‡‡	9.90 ± 1.77a‡, a‡‡
	CT	2.61 ± 1.22a‡, a‡‡	5.59 ± 0.16a‡, b‡‡	1.03 ± 0.01b‡, a‡‡	1.35 ± 0.27a‡, a‡‡	7.97 ± 0.12a‡, a‡‡
DS	CC	8.08^a‡, a‡‡	15.92^a‡, a‡‡	7.51^a‡, c‡‡	2.36^a‡, c‡‡	25.79^a‡, b‡‡
	CT	6.13 ± 0.21a‡, a‡‡	8.45 ± 0.32b‡, c‡‡	7.25 ± 2.10a‡, a‡‡	2.31 ± 0.69a‡, a‡‡	18.01 ± 2.46a‡, b‡‡
Test period	CC	5.52 ± 0.84	7.70 ± 1.20	2.16 ± 0.36	1.71 ± 0.21	11.57 ± 1.63
	CT	2.77 ± 0.70	4.84 ± 0.10	1.39 ± 0.27	1.72 ± 0.22	7.95 ± 0.39

* Including the cPOM and LF fractions.
** Including the physically protected (as defined in the Section 2.3. Soil carbon fractionation), the physically-chemically protected, and the bio-physically-chemically protected fractions (iPOM, H-μSilt + μClay, and NH-μSilt + μClay).
† Including H-dSilt + dClay.
†† Including NH-dSilt + dClay.
‡ ANOVA between the different treatments within the same soil moisture regime.
‡‡ ANOVA between the plots with the same treatment during the different soil moisture regimes; ^ the standard error of the mean cannot be calculated because sediment was only collected in one of the four rainfall events.

pattern of both sediment yield per TIP or event and per erosivity were similar to that of other studies in Mediterranean-climate areas (e.g. Marques et al., 2010; Biddoccu et al., 2017); with relatively low values of both metrics during autumn, the highest with some peaks during late autumn-early winter, and very low or lacking after May until the following hydrological season. Although the plots seeded with *Lolium multiflorum* tended to have the lowest sediment yield, there was no significant difference between the two temporary cover crops types. Therefore, the two types of CC communities provided similar ground cover (data already published by Gómez et al., 2018a,b), mainly by plant residues from the previous spring or by living plants from about early winter, to reduce the interrill erosion by intercepting the raindrops and dissipating impact energy.

The relatively few studies measuring soil erosion in woody orchards with different cover crops species with natural rainfall have shown contrasting results. Ruiz-Colmenero et al. (2013) using microplots (4 × 0.5 m) in a vineyard found significantly higher sediment losses (cumulative value of 4 years) in the *Brachypodum distachyon* treatment as compared to the *Secale cereale* cover crops. Using a similar design, with microplots as well (2 × 0.5 m), Sastre et al. (2017) found no differences

Table 7
Mean weighted annual sediment/soil carbon enrichment ratios (ER) of the non-protected and protected organic carbon fractions in the CC and CT plots. No significant difference –at 0.05 level– appeared between the two treatments at any fraction.

	Non-protected*	Protected				SOC
		Physically**	Chemically†	Bio-Chemically††	Total	Total
CC	0.87	1.37	0.64	1.01	1.08	1.00
CT	0.82	1.23	0.45	1.36	0.96	0.92
P-value	*0.846*	*0.698*	*0.314*	*0.174*	*0.614*	*0.623*

* Including the cPOM and LF fractions.
** Including the physically protected (as defined in the Section 2.3. Soil carbon fractionation), the physically-chemically protected, and the bio-physically-chemically protected fractions (iPOM, H-μSilt + μClay, and NH-μSilt + μClay).
† Including H-dSilt + dClay.
†† Including NH-dSilt + dClay.

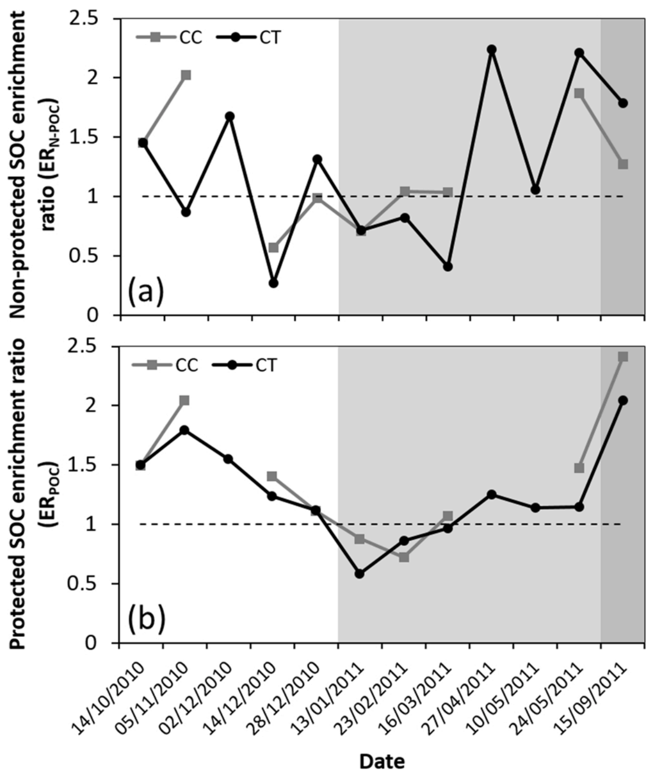

Fig. 6. Mean sediment/soil carbon enrichment ratios of non-protected (ER_{N-POC}; a) and protected (ER_{POC}; b) SOC fractions in the CC and CT plots in the 12 time-integrated periods. The white, light grey and dark grey areas correspond to the heavy-rainy (HRS), rainy (RS) and dry (DS) seasons.

in 4-year cumulative sediment losses between *Hordeum vulgare* and *Brachypodum distachyon* or between *Hordeum vulgare* and *Onobrychis viciifolia* Scop., however, with *Brachypodum distachyon* the cumulative sediment losses was the lowest.

At a larger scale (plots of 5 × 10 m), but under simulated rainfall, Repullo -Ruibérriz de Torres et al. (2018) compared runoff and sediment yield for two years in six different ground managements: tillage, spontaneous vegetation and sown cover crops of I) *Brachypodium distachyon*, II) *Sinapis alba*, III) *Vicia sativa*, and IV) *Vicia ervilia*. They concluded that CC significantly reduced erosion irrespectively of the plant species at the end of the trial, being the architecture of the surface cover a key issue to explore. Due to establishment problems of *B. distachyon* and *V. sativa* soil protection was lower compared to other CC the first year, contrasting to the results of Ramírez-García et al. (2015), who reported after a two-season study under field conditions a better ground cover during the developing stage of gramineous compared to leguminous and cruciferous.

The result in our one-year hydrological study showing no significant differences in sediment yield between the two types of seeded CC, is in line with some previous studies, highlighting that differences among CC species on soil protection might be site, and year, dependent in terms of species emergence and biomass development.

The averaged 55.6 % of annual reduction of SY under temporary CC compared to the uncovered soil agrees well, although at the lower end, with a number of studies that have showed, in other woody crops and under Mediterranean climate, a reduction in the sediment yield. Temporary CC along the alleys have shown a consistent effect in reducing soil losses in olives, vineyards and almonds. Gómez et al. (2011) in an analysis of a 3-year experiment across olives and vineyards in Spain, Portugal and France found that sediment losses in fields with temporary CC were in the range of 2 %–47 % of that generated in bare soil managed treatments. Martínez-Raya et al. (2006) measured in an almond orchard on a 35 % slope over a 4-year period soil losses with temporary CC of barley and lentils of 32 %–43 %, respectively, of those measured on the bare soil treatment; and Martínez-Mean et al. (2020) measured decreases in soil erosion of 85 % in almond orchards under reduced tillage combined with green manure. The relatively low percentage of reduction of this study compared to others was likely due to the relatively high erosivity (EI_{30}) in December, a period of time when living plants were not fully established after seeding which also disturbed the soil and reduced ground cover. Interestingly, during the first rainfall of 54.5 mm of early autumn, SY was significantly reduced in the seeded plots, despite that living plants were not fully developed, highlighting the positive effect of plant residues (Sastre et al., 2017) in reducing soil erosion, at least when EI_{30} is relatively low. This result agrees with that of Francia-Martínez et al. (2006) in an olive grove and with the field observations made by Napoli et al. (2017) in vineyards in central Italy, where permanent grass cover reduced significantly runoff during copious and intense rainfalls. López-Vicente et al. (2020) also found in vineyards in NE Spain, significant differences between the concentration of organic matter in sediment in the months with low and moderate-to-high ground cover.

4.2. Temporary seeded cover crops increase SOC fractions

The implementation of temporary CC not only reduced SY but also significantly increased the SOC content of the top 5 cm soil. Indeed, total SOC concentration after six years of temporary CC was significantly higher (by 48 %) than that of the CT plots. Similar results were obtained for a number of studies in olive groves (Nieto et al., 2013) and other woody crops, such as vineyards (Ruiz-Colmenero et al., 2013) and almonds (Ramos et al., 2010; Almagro et al., 2017). The higher SOC stock in soils under cover crop treatment was mainly due to the annual organic carbon input of the plant residues (measured as dry weight equivalent; DW). Vicente-Vicente et al. (2017) found an average net annual aboveground organic carbon input of 0.56 Mg DW ha^{-1} in ten olive groves with temporary spontaneous cover crop. However, the reported net annual organic carbon input into the soils by seeded CC are sometimes higher. For instance, Repullo-Ruibérriz de Torres et al. (2012) found during a two-year study a net aboveground annual C input of between 0.40 and 2.1 Mg DW ha^{-1}, depending on the seeded herbaceous species. In addition to the annual organic carbon input, the reduction in annual SOC losses by soil erosion (see below) also contributes to the increased of total SOC in the top 5 cm soil layer. Finally, plant residues together with the increase in micro-habitat diversity –provided by both residues and living plants under CC– might have an important impact on SOC accrual in our CC plots. That it can improve the ability of soil microbial communities to rapidly process plant residues and protect them in aggregates, and also introduces greater diversity of organic carbon compounds into the soil, some of which may be more resistant to decomposition (Tiemann et al., 2015).

Both, unprotected and protected SOC fractions were significantly higher under CC plots compared to bare tilled soils. The highest increase was achieved for the cPOM (the coarse non-protected SOC). This result was similar to that of Vicente-Vicente et al. (2017) who also analysed the SOC fractions in 10 olive groves with spontaneous temporary CC and other 10 comparable uncovered groves. The fact that in the top 5 cm soil, cPOM, but also LF, were significantly higher in the CC plots, was not unexpected as these fractions are mainly fed by partially decomposed plant residues (Six et al., 2000, 2002).

For the protected SOC fractions, although only the biochemically protected C of the silt + clay soil fractions were significantly higher, the physically protected C (iPOM) and the chemically protected C within microaggregates were 40 % and 41 % higher under CC. The higher physically protected C is due to the physical protection exerted by macro- and/or microaggregates on SOC, which is attributed to the compartmentalization of substrate and microbial biomass (Killham et al., 1993) and the reduced diffusion of oxygen into macro and, especially microaggregates, resulting in a reduced activity within the aggregates (Sollins et al., 1996). In our study, the macroaggregates stability of soils of CC were, on average, 1.52 times higher than that of the CT plots, which agrees with the recent findings of Garcia-Franco et al. (2015) who showed, after 4 years of green manuring in an almond orchard, that formation of micro- and macro-aggregates were promoted. Plant residues serve, following the decomposition process, as a binding agent to hold soil particles together forming aggregates (Jastrow et al., 1998), which might explain the higher macroaggregate stability and the increased content of SOC physically protected in the CC plots. In addition, the fact that the SOC of the silt + clay particles (<53 μm) within micro aggregates (53–250 μm) was higher in plant covered soil, suggests that SOC chemically protected within the microaggregates, and eventually stability of the microaggregates, is increased after the incorporation of plant cover residues, as reported by Six et al. (2000). This could be explained by the fact that the release of biogenic products and other binding agents, such as polysaccharides and root exudates (Puget and Drinkwater, 2001), during the incorporation and relatively rapid decomposition of the residues of the plant cover, may have promoted the solid-phase reaction between organic matter and clay and silt particles. These processes led to an increase in the chemically protected SOC within a SOC fraction that is physically protected, and to the formation of stable microaggregates (Golchin et al., 1994). Our results suggest that a significant part of the SOC stabilization is due to physico-chemical protection of organic carbon by mineral particles (Krull et al., 2003; Bronick and Lal, 2005). This result is in line with those obtained by Garcia-Franco et al. (2015) who found that the proportion of micro-aggregates, and its stability, within small macro-aggregates increased after green manuring together with reduced tillage. The higher SOC concentration in the silt + clay-occluded SOC in micro-aggregates of CC plots relative to CT, can be beneficial to long-term C sequestration because micro-aggregates have longer turnover times and higher stability than macro-aggregates (Denef et al., 2001; Huang et al., 2010), indicating the potential of this management practice to promote SOC accrual and stabilization.

The pool of biochemically protected carbon indicates the biochemical stabilization of organic carbon through biotic and abiotic creation of decay-resistant organic compounds, and is usually referred to as the passive or recalcitrant pool of SOC (Tan et al., 2004). The pool of biochemically protected carbon within the 53–250 μm aggregates were significantly higher in the top 5 cm of soil under CC. Therefore, the above and belowground residues of the temporary seeded cover crops are the source of a more complex chemical composition of the organic carbon and/or boost the conditions for the condensation and complexation of organic matter decomposition, rendering them more resistant to subsequent decomposition (Six et al., 2002). Therefore, at the regional scale of Andalusia, where olive groves represent a very high proportion of cropland, the use of plant cover is a promising practice that promotes the accumulation of protected SOC fractions, and thus, of C sequestration.

4.3. Preferential loss of SOC fractions under contrasted soil management

The CT plots lost on average 0.221 Mg C ha^{-1} during the studied hydrological cycle, whereas figure for the CC plots averaged 66 % of that (0.148 Mg C ha^{-1}). The values were similar to the grand mean of 0.140 Mg C ha^{-1} measured in runoff plots of three sites within an annual rainfall of between 360–550 mm ha^{-1} and during 1–5 hydrological cycles under Mediterranean climate (Roose and Barthès, 2006). Despite the significant difference in annual sediment yield between managements, annual eroded organic C was not significantly different. This was due to the higher organic carbon concentration of the sediment of CC (1.70 % ± 0.31) compared to the CT plots (1.07 % ± 0.03) and the high variability in sediment yield of the CC plots (coefficient of variation of 41 %). This finding agrees with Morsli et al. (2006) observations in a vertic soil, where sediment yield was twice under bare soil conditions than under cultivated with wheat, although eroded organic carbon was similar in both treatments because of sediment organic carbon concentration was twice in the cultivated soil.

The average retention of 73.1 kg C_{org} ha^{-1} yr^{-1} under cover crop compared to the bare soil in this relatively rainy hydrological cycle season, and under unfavourable conditions for soil protection by the cover crop, highlights the relative importance of considering eroded SOC in C budgets and C footprint analysis in olive groves. For instance, this amount of retained organic carbon is equivalent to the 30.7 % of the mean of organic carbon annually retained in one hectare in the stable structures (above and belowground olive tree biomass) of traditional olive groves (López-Bellido et al., 2016) or 13.05 % of the mean annual organic carbon input by spontaneous temporary CC measured by Vicente-Vicente et al. (2017).

This organic carbon which is retained within the agroecosystem due to the sediment yield reduction, together with the annual input of organic carbon due to the above and belowground biomass of the temporary seeded CC, not only explains the higher SOC content of the top soil layer under CC compared to CT, but also confirms the important role of CC on SOC accumulation in woody crops.

In both managements, the contribution of protected carbon to the total eroded C was the highest. Within this pool, the physically protected fraction (53–250 μm excluding the LF fraction) was the one that contributed the most. Most of the soil particles in soil of CC ($\bar{x}$ = 66.4 %) and CT ($\bar{x}$ = 63.1 %) plots were between 53–250 μm and were not significantly different among the treatments, and nor between the soil and sediment samples when comparing samples from the same treatment (Supplementary Table 1). Similarly, the content of the 53–250 μm sized particle of the sediment collected in the CC ($\bar{x}$ = 65.6 %) and CT ($\bar{x}$ = 64.3 %) plots was the highest. Therefore, the particle size distribution of the sediments –during the whole studied period– resembles that of the soil, independently of the management. This result contrasts with the relatively common assumption that clay and silt sized sediments are preferably transported by runoff, typically resulting in clay (ER_{clay}) and silt (ER_{silt}) enrichment ratios >1 (Warrington et al., 2009), although this is highly dependent on soil properties, slope, erosion dominant processes, and erosion and rainfall intensity, among others. The fact that in our study the range of fine sand sized particles in the sediment, and thus the organic carbon in this particle size range, was the most abundant –as it was in the soils– could be explained because 79.7 % and 70.3 % of the total SY in the CC and CT, respectively, took place in only one month (TIPs #4, 5 and 6). In this month –December 2010– the cumulative EI_{30} was higher than 105.6 MJ mm ha^{-1} h^{-1}. Under this relatively high EI_{30} and when soil was subjected to a cumulative rainfall of 166 mm during the previous two months, some of the microaggregates detached resulting in a nonselective erosion process. Thus, during this period of high SY, the presence of the CC clearly reduced the magnitude of soil erosion, but did not affect the selectiveness of soil particle transport. Establishment of the cover in early fall is a critical period, since its opens a "window of opportunity" for erosion while the soil is bare before the plants emerge and provide ground cover. For this reason, fast growing species which emerge early in fall and have the possibility of self-seeding over multiple years have been recommended to minimize this risk (Gómez and Soriano, 2020; Gómez, 2017).

The amount of non-protected carbon lost did not differ between management, despite that the sediment yield did. This was so because there were 1.75 and 2.7 times more cPOM and LF in the top 5 cm of soils of CC compared to CT plots, resulting in higher carbon content of the LF and cPOM in the sediment of the CC plots, especially in TIPs previous to December, when $ER_{N\text{-}POC}$ was close to 2.0. Indeed, an $ER_{SOC} > 1$ in sediment eroded under low rainfall intensity and plant covered soil has been often attributed to poorly decomposed non-cohesive plant fragments (Ghadiri and Rose, 1991; Martínez-Mena et al., 2012), non-protected carbon in our study, which, despite their relatively low concentration in the soil, are transported preferentially due to their low density. Indeed, the presence of a thick litter layer in early autumn in the CC plots could reduce flow velocity; hence, the detachment and transport capacities of the runoff flow, by provided easily transportable organic particles. Despite this selectivity in losing organic carbon in the CC plots, generally was not significant with respect to CT plots because the contribution of the sediment lost during this period of low SY to the total was very low.

Overall, the ER_{SOC} and the ER of the C_{org} fractions of different protective levels of the sediment were not significantly different from 1 and the presence of the seeded temporary CC did not affect significantly the ER_{SOC}. This disagrees with other studies that have found that ER_{SOC} of sediment from plots with vegetation is usually higher than 1 and higher than comparable bare soils. For instance, ER_{SOC} was the lowest and close to 1 for bare soils, and the highest (>2) were achieved in plots cultivated with herbaceous plants or with scrubs (Morsli et al., 2006). Roose and Barthès (2006) found that ER_{SOC} under natural vegetation was typically higher than 2.4, whereas for bare tilled soils were typically around 1.0. The ER_{SOC} close to 1 and the lack of effects of the presence of the cover crop in the ER_{SOC} of our study were likely due to the very high proportion of the annual sediment yield of December with high erosion rates, and development of some micro-rills, which fully mixed the transported topsoil. This is in line with some studies that have found that the higher the rainfall intensity and sediment yield are, the lower is the ER_{SOC}. For instance, Roose and Barthès (2006) found in 54 runoff plots in tropical and Mediterranean regions that the highest (>3) and the smallest (1) ER_{SOC} were measured on plots under vegetation with low or very low (<0.5 Mg ha^{-1} y^{-1}) and high (>20 Mg ha^{-1} y^{-1}) soil erosion respectively. In the same line, Wilken et al. (2017) recently showed, using an event-based multi-class sediment transport model, that the higher the suspended sediment concentration the lower is the ER_{SOC} with values around 1 when suspended sediment concentration was above the threshold of 30 g L^{-1}. Therefore, under high rainfall intensity in a period when seeded, or spontaneous, temporary CC are not fully stablished, erosion does not show preferences in the eroded SOC.

5. Conclusions

Temporary cover crops are key to increase total SOC and fractions of different protection levels in woody orchards, such as olive groves. The higher total (+46 %), unprotected (+88.4 %) and protected (+28.5 %) SOC contents in the top –5 cm– soil layer under six year of CC highlights the effectiveness of this agricultural management practice to sequester C in the topsoil of permanent crops.

Temporary cover crops were also an effective strategy to reduce the sediment yield although in the year of our experiment, annual rates were still above the tolerable rate of soil loss for croplands due to concentration of rainfall events during the key months of implementation of the seeded cover crops. The average retention within the agroecosystem of 73.1 kg C_{org} ha^{-1} yr^{-1} with the presence of the temporary cover crops, as compared to bare soil, during this rainy hydrological cycle season indicates the relative importance of considering eroded SOC in C budgets and C footprint analysis in olive groves. The presence of the temporary cover crops in this olive grove did not result in preferential loss of a particular C_{org} fraction as enrichment ratios of protected and non-protected C_{org} did not differ significantly between managements and from 1.

The fact that a great percentage (>70 %) of the annual sediment yield was eroded in one month (December) with high EI_{30} but little vegetation ground cover limited the effectiveness of this management in reducing the sediment yield and in increasing C_{org} retention. In addition, this asynchrony between the periods of full development of the CC plants and those with the highest rainfall erosivity prevented any selectiveness of the eroded C_{org}. Thus, more efforts should be paid on searching for CC plant species of fast-growing short life-cycle that emerge early in fall to maximize soil retention and species with self-seeding capacity on undisturbed soil, eliminating soil preparation for sowing and protecting soil surface with plant residues from the previous season.

Declaration of Competing Interest

The authors declare that they have no known competing financial interests or personal relationships that could have appeared to influence the work reported in this paper.

Acknowledgements

This research has been supported by the Spanish Government (grants no. AGL2015-40128-C03-01 and PID2019-105793RB-I00), FEDER funds and the European Commission (SHui, grant no. 773903) and the H2020 PRIMA project SUSTAINOLIVE (grant no. 1811).

Appendix A. Supplementary data

Supplementary material related to this article can be found, in the online version, at doi:https://doi.org/10.1016/j.still.2021.105119.

References

Almagro, M., Garcia-Franco, N., Martínez-Mena, M., 2017. The potential of reducing tillage frequency and incorporating plant residues as a strategy for climate change mitigation in semiarid Mediterranean agroecosystems. Agric. Ecosyst. Environ. 246, 210–220. https://doi.org/10.1016/j.agee.2017.05.016.

Anderson, J., Ingram, J., 1993. Soil organic matter and organic carbon. Tropical Soil Biology and Fertility: A Handbook of Methods. CAB International, Oxford, UK, pp. 171–221.

Beaufoy, G., 2001. EU Policies for Olive Farming: Unsustainable on all Counts. BirdLife International, WWF, Brussels.

Ben-Salem, N., Álvarez, S., López-Vicente, M., 2018. Soil and water conservation in rainfed vineyards with common sainfoin and spontaneous vegetation under different ground conditions. Water 10 (8), 1058. https://doi.org/10.3390/w10081058.

Biddoccu, M., Ferraris, S., Pitacco, A., Cavallo, E., 2017. Temporal variability of soil management effects on soil hydrological properties, runoff and erosion at the field scale in a hillslope vineyard, North-West Italy. Soil Tillage Res. 165, 46–58. https://10.1016/j.still.2016.07.017.

Boix-Fayos, C., de Vente, J., Albaladejo, J., Martínez-Mena, M., 2009. Soil carbon erosion and stock as affected by land use changes at the catchment scale in Mediterranean ecosystems. Agric. Ecosyst. Environ. 133 (1–2), 75–85. https://doi.org/10.1016/j.agee.2009.05.013.

Borrelli, P., Panagos, P., Lugato, E., Alewell, C., Ballabio, C., Montanarella, L., Robinson, D.A., 2018. Lateral carbon transfer from erosion in noncroplands matters (Letters to Editor). Glob. Change Biol. 24 (8), 3283–3284. https://doi.org/10.1111/gcb.14125.

Bronick, C.J., Lal, R., 2005. Soil structure and management: a review. Geoderma 124, 3–22. https://doi.org/10.1016/j.geoderma.2004.03.005.

Denef, K., Six, J., Bossuyt, H., Frey, S.D., Elliott, E.T., Merckx, R., Paustian, K., 2001. Influence of dry-wet cycles on the interrelationship between aggregate, particulate organic matter, and microbial community dynamics. Soil Biol. Biochem. 33, 1599–1611. https://doi.org/10.1016/S0038-0717(01)00076-1.

Francia-Martínez, J.R., Durán-Zuazo, V.H., Martínez-Raya, A., 2006. Environmental impact from mountainous olive orchards under different soil-management systems (SE Spain). Sci. Total Environ. 358 (1–3), 46–60. https://doi.org/10.1016/j.scitotenv.2005.05.036.

Garcia-Franco, N., Albaladejo, J., Almagro, M., Martínez-Mena, M., 2015. Beneficial effects of reduced tillage and green manure on soil aggregation and stabilization of organic carbon in a Mediterranean agroecosystem. Soil Till. Res. 153, 66–75. https://doi.org/10.1016/j.still.2015.05.010.

Ghadiri, H., Rose, C., 1991. Sorbed chemical transport in overland flow: II. Enrichment ratio variation with erosion processes. J. Environ. Qual. 20, 634–641. https://doi.org/10.2134/jeq1991.00472425002000030021x.

Golchin, A., Oades, J.M., Skjemstad, J.O., Clarke, P., 1994. Study of free and occluded particulate organic matter in soils by solid state ^{13}C Cp/MAS NMR spectroscopy and scanning electron microscopy. Aust. J. Soil Res. 32, 285–309. https://doi.org/10.1071/SR9940285.

Gómez, J.A., 2017. Sustainability using cover crops in Mediterranean tree crops, olives and vines – challenges and current knowledge. Hung. Geogr. Bull. 66 (1), 13–28. https://doi.org/10.15201/hungeobull.66.1.2.

Gómez, J.A., Soriano, M.A., 2020. Evaluation of the suitability of three autochthonous herbaceous species as cover crops under Mediterranean conditions through the calibration and validation of a temperature-based phenology model. Agric. Ecosyst. Environ. 291, 106788 https://doi.org/10.1016/j.agee.2019.106788.

Gómez, J.A., Guzmán, M.G., Giráldez, J.V., Fereres, E., 2009. The influence of cover crops and tillage on water and sediment yield, and on nutrient, and organic matter losses in an olive orchard on a sandy loam soil. Soil Till. Res. 106 (1), 137–144. https://doi.org/10.1016/j.still.2009.04.008.

Gómez, J.A., Llewellyn, C., Basch, G., Sutton, P.B., Dyson, J.S., Jones, C.A., 2011. The effects of cover crops and conventional tillage on soil and runoff loss in vineyards and olive groves in several Mediterranean countries. Soil Use Manag. 27 (4), 502–514. https://doi.org/10.1111/j.1475-2743.2011.00367.x.

Gómez, J.A., Francia, J.R., Guzmán, G., Vanwalleghem, T., Durán-Zuazo, V.H., Castillo, C., Aranda, M., Cárceles, B., Moreno, A., Torrent, J., Barrón, V., 2017. Lateral transfer of organic carbon and phosphorus by water erosion at hillslope scale in Southern Spain olive orchards. Vadose Zone J. 16 (12), 1–15. https://doi.org/10.2136/vzj2017.02.0047.

Gómez, J.A., Campos, M., Guzmán, G., Castillo-Llanque, F., Vanwalleghem, T., Lora, Á., Giráldez, J.V., 2018a. Soil erosion control, plant diversity, and arthropod communities under heterogeneous cover crops in an olive orchard. Environ. Sci. Pollut. Res. 25 (2), 977–989. https://doi.org/10.1007/s11356-016-8339-9.

Gómez, J.A., Campos, M., Guzmán, G., Castillo-Llanque, F., Vanwalleghem, T., Lora, Á., Giráldez, J.V., 2018b. Soil erosion control, plant diversity, and arthropod communities under heterogeneous cover crops in an olive orchard. Environ. Sci. Pollut. Res. 25 (2), 977–989. https://doi.org/10.1007/s11356-016-8339-9.

Gómez, J.A., Guzmán, G., Toloza, A., Resch, C., García-Ruíz, R., Mabit, L., 2020. Variation of soil organic carbon, stable isotopes, and soil quality indicators across an erosion–deposition catena in a historical Spanish olive orchard. SOIL 6, 179–194. https://doi.org/10.5194/soil-6-179-2020.

Guzmán, G., Barrón, V., Gómez, J.A., 2010. Evaluation of magnetic iron oxides as sediment tracers in water erosion experiments. Catena 82 (2), 126–133. https://doi.org/10.1016/j.catena.2010.05.011.

Guzmán, G., Cabezas, J.M., Sánchez-Cuesta, R., Lora, Á., Bauer, T., Strauss, P., Winter, S., Zaller, J.G., Gómez, J.A., 2019a. A field evaluation of the impact of temporary cover crops on soil properties and vegetation communities in Southern Spain vineyards. Agric. Ecosyst. Environ. 277, 135–145. https://doi.org/10.1016/j.agee.2018.11.010.

Guzmán, G., Perea-Moreno, A.J., Gómez, J.A., Cabrerizo-Morales, M.A., Martínez, G., Giráldez, J.V., 2019b. Water related properties to assess soil quality in two olive orchards of South Spain under different management strategies. Water 11 (2), 367. https://doi.org/10.3390/w11020367.

Huang, Y., Sun, W.J., Zhang, W., Yu, Y.Q., 2010. Changes in soil organic carbon of terrestrial ecosystems in China: a mini review. Sci. China Life Sci. 53, 766–775. https://doi.org/10.1007/s11427-010-4022-4.

Jastrow, J.D., Miller, R.M., Lussenhop, J., 1998. Contributions of interacting biological mechanisms to soil aggregate stabilization in restored prairie. Soil Biol. Biochem. 30, 905–916. https://doi.org/10.1016/S0038-0717(97)00207-1.

Jian, J., Du, X., Reiter, M.S., Stewart, R.D., 2020. A meta-analysis of global cropland soil carbon changes due to cover cropping. Soil Biol. Biochem. 143, 107735 https://doi.org/10.1016/j.soilbio.2020.107735.

Killham, K., Amato, M., Ladd, J., 1993. Effect of substrate location in soil and soil porewater regime on carbon turnover. Soil Biol. Biochem. 25 (1), 57–62. https://doi.org/10.1016/0038-0717(93)90241-3.

Krull, E.S., Baldock, J.A., Skjemstad, J.O., 2003. Importance of mechanisms and processes of the stabilization of soil organic matter for modelling carbon turnover. Funct. Plant Biol. 30, 207–222. https://doi.org/10.1071/FP02085.

Lal, R., 2003. Soil erosion and the global carbon budget. Environ. Int. 29 (4), 437–450. https://doi.org/10.1016/S0160-4120(02)00192-7.

Lal, R., 2004. Soil carbon sequestration to mitigate climate change. Geoderma 123 (1-2), 1–22. https://doi.org/10.1016/j.geoderma.2004.01.032.

Lal, R., 2019. Accelerated soil erosion as a source of atmospheric CO_2. Soil Till. Res. 188, 35–40. https://doi.org/10.1016/j.still.2018.02.001.

Li, T., Zhang, H., Wang, X., Cheng, S., Fang, H., Liu, G., Yuan, W., 2019. Soil erosion affects variations of soil organic carbon and soil respiration along a slope in Northeast China. Ecol. Process. 8, 28. https://doi.org/10.1186/s13717-019-0184-6.

López-Bellido, P.J., López-Bellido, L., Fernandez-Garcia, P., Muñoz-Romero, V., López-Bellido, F.J., 2016. Assessment of carbon sequestration and the carbon footprint in olive groves in Southern Spain. Carbon Manag. 7, 161–170. https://doi.org/10.1080/17583004.2016.1213126.

López-Vicente, M., García-Ruiz, R., Guzmán, G., Vicente-Vicente, J.L., Van Wesemael, B., Gómez, J.A., 2016. Temporal stability and patterns of runoff and runon with different cover crops in an olive orchard (SW Andalusia, Spain). Catena 147, 125–137. https://doi.org/10.1016/j.catena.2016.07.002.

López-Vicente, M., Calvo-Seas, E., Álvarez, S., Cerdà, A., 2020. Effectiveness of cover crops to reduce loss of soil organic matter in a rainfed vineyard. Land 9 (7), 230. https://doi.org/10.3390/land9070230.

Lugato, E., Paustian, K., Panagos, P., Jones, A., Borrelli, P., 2016. Quantifying the erosion effect on current carbon budget of European agricultural soils at high spatial resolution. Glob. Change Biol. 22 (5), 1976–1984. https://doi.org/10.1111/gcb.13198.

Marques, M.J., García-Muñoz, S., Muñoz-Organero, G., Bienes, R., 2010. Soil conservation beneath grass cover in hillside vineyards under Mediterranean climatic conditions (Madrid, Spain). Land Degrad. Dev. 21 (2), 122–131. https://doi.org/10.1002/ldr.915.

Martínez-Mean, M., Carrillo-López, E., Boix-Fayos, C., Almagro, M., García Franco, N., Díaz-Pereira, E., Montoya, I., de Vente, J., 2020. Lont-term effectiveness of sustainable land management practices to control runoff, soil erosion, and nutrient loss and the role of rainfall intensity in Mediterranean rainfed agroecosystems. Catena 187, 104352. https://doi.org/10.1016/j.catena.2019.104352.

Martínez-Mena, M., López, J., Almagro, M., Albaladejo, J., Castillo, V., Ortiz, R., Boix-Fayos, C., 2012. Organic carbon enrichment in sediments: effects of rainfall characteristics under different land uses in a Mediterranean area. Catena 94, 36–42. https://doi.org/10.1016/j.catena.2011.02.005.

Martínez-Raya, A., Durán-Zuazo, V.H., Francia-Martínez, J.R., 2006. Soil erosion and runoff response to plant-cover strips on semiarid slopes (SE Spain). Land Degrad. Dev. 17, 1–11. https://doi.org/10.1002/ldr.674.

McGregor, K.C., Mutchler, C.K., 1976. Status of the R factor in northern Mississippi. In: Foster, G.R. (Ed.), Soil Erosion: Prediction and Control. Proc. Nat. Soil Erosion Conf. at Purdue University, Spec. Publ. No. 21. Soil Conserv. Soc. Am., Ankeny, Iowa, pp. 135–142 (393 PP).

Minasny, B., et al., 2017. Soil carbon 4 per mille. Geoderma 292, 59–86. https://doi.org/10.1016/j.geoderma.2017.01.002.

Morsli, B., Mazour, M., Arabi, M., Mededjel, N., Roose, E., 2006. Influence of land use, and cultural practices on erosion, eroded carbon, and soil carbon stocks at the plot scale in the Mediterranean mountains of northern Algeria. In: Roose, E., Lal, R., Feller, C., Barthès, B., Stewart, B.A. (Eds.), Soil Erosion and Carbon Dynamics. Taylor et Francis, Boca Raton, pp. 55–72 (Advances in Soil Science). Land Uses, Erosion and Carbon Sequestration: International Colloquium, Montpellier (FRA), 2002/09/23-28. ISBN 978-1-56670-688-2.

Naipal, V., Ciais, P., Wang, Y., Lauerwald, R., Guenet, B., Van Oost, K., 2018. Global soil organic carbon removal by water erosion under climate change and land use change during AD1850–2005. Biogeosciences 15, 4459–4480. https://doi.org/10.5194/bg-15-4459-2018.

Napoli, M., Dalla-Marta, A., Zanchi, C.A., Orlandini, S., 2017. Assessment of soil and nutrient losses by runoff under different soil management practices in an Italian hilly vineyard. Soil Tillage Res. 168, 71–80. https://doi.org/10.1016/j.still.2016.12.011.

Nearing, M.A., Yin, S., Borrelli, P., Polyakov, V.O., 2017. Rainfall erosivity: an historical review. Catena 157, 357–362. https://doi.org/10.1016/j.catena.2017.06.004.

Nieto, O.M., Castro, J., Fernández-Ondoño, E., 2013. Conventional tillage versus cover crops in relation to carbon fixation in Mediterranean olive cultivation. Plant Soil 365 (1–2), 321–335. https://doi.org/10.1007/s11104-012-1395-0.

Novara, A., Minacapilli, M., Santoro, A., Rodrigo-Comino, J., Carrubba, A., Sarno, M., Venezia, G., Gristina, L., 2019. Real cover crops contribution to soil organic carbon sequestration in sloping vineyard. Sci. Total Environ. 652, 300–306. https://doi.org/10.1016/j.scitotenv.2018.10.247.

Ogle, S.M., Alsaker, C., Baldock, J., Bernoux, M., Breidt, F.J., McConkey, B., Regina, K., Vazquez-Amabile, G.G., 2019. Climate and soil characteristics determine where no-till management can store carbon in soils and mitigate greenhouse gas emissions. Sci. Rep. 9 (1), 11665 https://doi.org/10.1038/s41598-019-47861-7.

Paustian, K., Six, J., Elliott, E.T., Hunt, H.W., 2000. Management options for reducing CO_2 emissions from agricultural soils. Biogeochemistry 48, 147–163. https://doi.org/10.1023/A:1006271331703.

Plante, A.F., Conant, R.T., Paul, E.A., Paustian, K., Six, J., 2006. Acid hydrolysis of easily dispersed and microaggregate-derived silt- and clay-sized fractions to isolate resistant soil organic matter. Eur. J. Soil Sci. 57 (4), 456–467. https://doi.org/10.1111/j.1365-2389.2006.00792.x.

Puget, P., Drinkwater, L.E., 2001. Short-term dynamics of root- and shoot-derived carbon from a leguminous green manure. Soil Sci. Soc. Am. J. 65, 771–779. https://doi.org/10.2136/sssaj2001.653771x.

Ramírez-García, J., Gabriel, J.L., Alonso-Ayuso, M., Quemada, M., 2015. Quantitative characterization of five cover crop species. J. Agric. Sci. 153, 1174–1185. https://doi.org/10.1017/S0021859614000811.

Ramos, M.E., Benítez, E., García, P.A., Robles, A.B., 2010. Cover crops under different managements vs. frequent tillage in almond orchards in semiarid conditions: effects on soil quality. Appl. Soil Ecol. 44 (1), 6–14. https://doi.org/10.1016/j.apsoil.2009.08.005.

Repullo-Ruibérriz de Torres, M.A., Carbonell, R., Alcántara, C., Rodríguez-Lizana, A., Ordóñez, R., 2012. Carbon sequestration potential of residues of different types of cover crops in olive groves under Mediterranean climate. Span. J. Agric. Res. 10 (3), 649–661. https://doi.org/10.5424/sjar/2012103-562-11.

Repullo-Ruibérriz de Torres, M.A., Ordóñez-Fernández, R., Giráldez, J.V., Márquez-García, J., Laguna, A., Carbonell-Bojollo, R., 2018. Efficiency of four different seeded plants and native vegetation as cover crops in the control of soil and carbon losses by water erosion in olive orchards. Land Degrad. Dev. 29 (8), 2278–2290. https://doi.org/10.1002/ldr.3023.

Rolando, J.L., Dubeux-Jr, J.C., Perez, W., Ramirez, D.A., Turin, C., Ruiz-Moreno, M., Comerford, N.B., Mares, V., Garcia, S., Quiroz, R., 2017. Soil organic carbon stocks and fractionation under different land uses in the Peruvian high-Andean Puna. Geoderma 307, 65–72. https://doi.org/10.1016/j.geoderma.2017.07.037.

Roose, E., Barthès, B., 2006. Soil carbon erosion and its selectivity at the plot scale in tropical and Mediterranean regions. In: Roose, E., Lal, R., Feller, C., Barthès, B., Stewart, B.A. (Eds.), Soil Erosion and Carbon Dynamics. Taylor et Francis, Boca Raton, pp. 55–72 (Advances in Soil Science). Land Uses, Erosion and Carbon Sequestration: International Colloquium, Montpellier (FRA), 2002/09/23-28. ISBN 978-1-56670-688-2.

Ruiz-Colmenero, M., Bienes, R., Eldridge, D.J., Marques, M.J., 2013. Vegetation cover reduces erosion and enhances soil organic carbon in a vineyard in the central Spain. Catena 104, 153–160. https://doi.org/10.1016/j.catena.2012.11.007.

Sastre, B., Barbero-Sierra, C., Bienes, R., Marques, M.J., García-Díaz, A., 2017. Soil loss in an olive grove in Central Spain under cover crops and tillage treatments, and farmer perceptions. J. Soil Sediment 17, 873–888. https://doi.org/10.1007/s11368-016-1589-9.

Scheidel, A., Krausmann, F., 2011. Diet, trade and land use: a socio-ecological analysis of the transformation of the olive oil system. Land Use Policy 28 (1), 47–56. https://doi.org/10.1016/j.landusepol.2010.04.008.

Six, J., Elliott, E., Paustian, K., 2000. Soil macroaggregate turnover and microaggregate formation: a mechanism for C sequestration under no-tillage agriculture. Soil Biol. Biochem. 32, 2099–2103. https://doi.org/10.1016/S0038-0717(00)00179-6.

Six, J., Conant, R.T., Paul, E.A., Paustian, K., 2002. Stabilization mechanisms of soil organic matter: implications for C-saturation of soils. Plant Soil 241 (2), 155–176. https://doi.org/10.1023/A:1016125726789.

Soil Survey Staff, 2014. Keys to Soil Taxonomy, 12th ed. USDA-Natural Resources Conservation Service, Washington, DC.

Sollins, P., Hoffman, P., Caldwell, B., 1996. Stabilization and destabilization of soil organic matter: mechanisms and controls. Geoderma 74 (1–2), 65–105. https://doi.org/10.1016/S0016-7061(96)00036-5.

Stewart, C.E., Paustian, K., Conant, R.T., Plante, A.F., Six, J., 2009. Soil carbon saturation: implications for measurable carbon pool dynamics in long-term incubations. Soil Biol. Biochem. 41 (2), 357–366. https://doi.org/10.1016/j.soilbio.2008.11.011.

Stockmann, U., et al., 2013. The knowns, known unknowns and unknowns of sequestration of soil organic carbon. Agric. Ecosyst. Environ. 164, 80–99. https://doi.org/10.1016/j.agee.2012.10.001.

Sykes, A.J., et al., 2020. Characterising the biophysical, economic and social impacts of soil carbon sequestration as a greenhouse gas removal technology. Glob. Change Biol. 26 (3), 1085–1108. https://doi.org/10.1111/gcb.14844.

Tan, Z.X., Lal, R., Izaurralde, R.C., Post, W.M., 2004. Biochemically protected soil organic carbon at the North Appalachian experimental watershed. Soil Sci. 169, 1–11. https://doi.org/10.1097/01.ss.0000131227.51226.68.

Tiemann, L., Grandy, A., Atkinson, E., Marin-Spiotta, E., McDaniel, M., 2015. Crop rotational diversity enhances belowground communities and functions in an agroecosystem. Ecol. Lett. 18, 761–771. https://doi.org/10.1111/ele.12453.

Vanwalleghem, T., Amate, J.I., de Molina, M.G., Fernández, D.S., Gómez, J.A., 2011. Quantifying the effect of historical soil management on soil erosion rates in Mediterranean olive orchards. Agric. Ecosyst. Environ. 142 (3–4), 341–351. https://doi.org/10.1016/j.agee.2011.06.003.

Vicente-Vicente, J.L., García-Ruiz, R., Francaviglia, R., Aguilera, E., Smith, P., 2016. Soil carbon sequestration rates under Mediterranean woody crops using recommended management practices: a meta-analysis. Agric. Ecosyst. Environ. 235, 204–214. https://doi.org/10.1016/j.agee.2016.10.024.

Vicente-Vicente, J.L., Gómez-Muñoz, B., Hinojosa-Centeno, M.B., Smith, P., Garcia-Ruiz, R., 2017. Carbon saturation and assessment of soil organic carbon fractions in Mediterranean rainfed olive orchards under plant cover management. Agric. Ecosyst. Environ. 245, 135–146. https://doi.org/10.1016/j.agee.2017.05.020.

Wang, X., Cammeraat, E.L.H., Cerli, C., Kalbitz, K., 2014. Soil aggregation and the stabilization of organic carbon as affected by erosion and deposition. Soil Biol. Biochem. 72, 55–65. https://doi.org/10.1016/j.soilbio.2014.01.018.

Wang, Y., Fang, N., Zhang, F., Wang, L., Wu, G.L., Yang, M., 2017a. Effects of erosion on the microaggregate organic carbon dynamics in a small catchment of the Loess Plateau, China. Soil Till. Res. 174, 205–213. https://doi.org/10.1016/j.still.2017.08.001.

Wang, Z., Hoffmann, T., Six, J., Kaplan, J.O., Govers, G., Doetterl, S., Van Oost, K., 2017b. Human-induced erosion has offset one-third of carbon emissions from land cover change. Nat. Clim. Change 7, 345–349. https://doi.org/10.1038/nclimate3263.

Warrington, D.N., Mamedov, A.I., Bhardwaj, A.K., Levy, G.J., 2009. Primary particle size distribution of eroded material affected by degree of aggregate slaking and seal development. Eur. J. Soil Sci. 60, 84–93. https://doi.org/10.1111/j.1365-2389.2008.01090.x.

Wiaux, F., Cornelis, J.T., Cao, W., Vanclooster, M., Van Oost, K., 2014. Combined effect of geomorphic and pedogenic processes on the distribution of soil organic carbon quality along an eroding hillslope on loess soil. Geoderma 216, 36–47. https://doi.org/10.1016/j.geoderma.2013.10.013.

Wilken, F., Sommer, M., Van Oost, K., Bens, O., Fiener, P., 2017. Process-oriented modelling to identify main drivers of erosion-induced carbon fluxes. SOIL 3, 83–94. https://doi.org/10.5194/soil-3-83-2017.

Xiao, H., Li, Z., Chang, X., Huang, B., Nie, X., Liu, C., Liu, L., Wang, D., Jiang, J., 2018. The mineralization and sequestration of organic carbon in relation to agricultural soil erosion. Geoderma 329, 73–81. https://doi.org/10.1016/j.geoderma.2018.05.018.